The concept of active site in heterogeneous catalysis

Charlotte Vogt[1,2] ✉ *and Bert M. Weckhuysen*[1] ✉

Abstract | Catalysis is at the core of chemistry and has been essential to make all the goods surrounding us, including fuels, coatings, plastics and other functional materials. In the near future, catalysis will also be an essential tool in making the shift from a fossil-fuel-based to a more renewable and circular society. To make this reality, we have to better understand the fundamental concept of the active site in catalysis. Here, we discuss the physical meaning — and deduce the validity and, therefore, usefulness — of some common approaches in heterogeneous catalysis, such as linking catalyst activity to a 'turnover frequency' and explaining catalytic performance in terms of 'structure sensitivity' or 'structure insensitivity'. Catalytic concepts from the fields of enzymatic and homogeneous catalysis are compared, ultimately realizing that the struggle that one encounters in defining the active site in most solid catalysts is likely the one we must overcome to reach our end goal: tailoring the precise functioning of the active sites with respect to many different parameters to satisfy our ever-growing needs. This article ends with an outlook of what may become feasible within the not-too-distant future with modern experimental and theoretical tools at hand.

Turnover frequency
The turnover frequency is defined as the turnover unit per time. For most industrial applications, the turnover frequency is 10^{-3}–10^{2}.

Structure sensitivity
A reaction in which not all surface sites have the same activity. The surface-normalized activity changes with nanoparticle size for structure-sensitive reactions.

[1]*Inorganic Chemistry and Catalysis, Debye institute for Nanomaterials, Utrecht University, Utrecht, Netherlands.*

[2]*Schulich Faculty of Chemistry, Technion – Israel Institute of Technology, Haifa, Israel.*

✉*e-mail: C.Vogt@technion.ac.il; B.M.Weckhuysen@uu.nl*

https://doi.org/10.1038/s41570-021-00340-y

The global revenue of the chemical industry in 2019 amounted to an approximate US$4 trillion[1], of which an estimated 85% involved catalytic processes[2]. Few things in catalysis are as important — yet, as elusive — as the concept of the active site. The active site is what makes a catalyst work. It brings, as we know from the landmark studies of Wilhelm Ostwald (1853–1932), Svante Arrhenius (1859–1927) and Jacobus van 't Hoff (1852–1911), the kinetics of a chemical reaction in disbalance. This generally lowers the activation energy and, thus, increases the speed of a desired chemical reaction, leaving the reaction's thermodynamics unaffected (FIG. 1a). Heterogeneous catalysis is a diverse and highly interdisciplinary field, which combines knowledge from materials and surface science, physical, analytical and theoretical chemistry, chemical engineering and, not least, organic and inorganic chemistry. By combining advanced knowledge in synthesis techniques[3–7], with strides in space-resolved and time-resolved analytical methods[8–12], as well as advanced theoretical knowledge for computational modelling[13–16], one can argue that we are at the doorstep to the era of rational catalyst and process design. Defining the 'active site' along with the various actors that determine its activity are the ingress to conceptualizing the necessary novel catalysts, concepts and processes to tackle some of the immense challenges modern society faces, such as the quest for an energy transition or a circular society aiding to abate climate change.

As such, in this Review, we discuss the physical meaning — and deduce the validity and, therefore, usefulness — of some common approaches in heterogeneous catalysis, such as linking catalyst activity to a 'turnover frequency' and explaining catalytic performance in terms of 'structure sensitivity' or 'structure insensitivity'. To do so, we borrow and compare catalytic concepts from the fields of enzymatic and homogeneous catalysis (for example, 'turnover number').

The active site in a solid catalyst

Paul Sabatier (1854–1941) stated that, in order for a catalyst (in his case, often a "finely divided metal") to work, the adsorbent should neither be adsorbed too strongly nor too weakly, an observation which, among others, earned him the 1912 Nobel Prize in Chemistry for his seminal work on hydrogenation catalysis[17–20]. Linus Pauling (1901–1994) added that the catalyst (in his case, an enzyme) must bind the transition state more tightly than the substrate[21]. These two concepts lie at the heart of catalysis at the active site, summarized in FIG. 1a. Yet, before we begin to analyse the active site in a bottom-up manner, we must be aware of the multidimensional factors across multiple scales that can contribute to the observed activity of the 'active site'. Heterogeneous catalysts often involve porosity on the micrometre to nanometre scale[22], and are subject to phase and morphological transformations over a huge time range from as long as years to as short as sub-milliseconds[11,23,24].

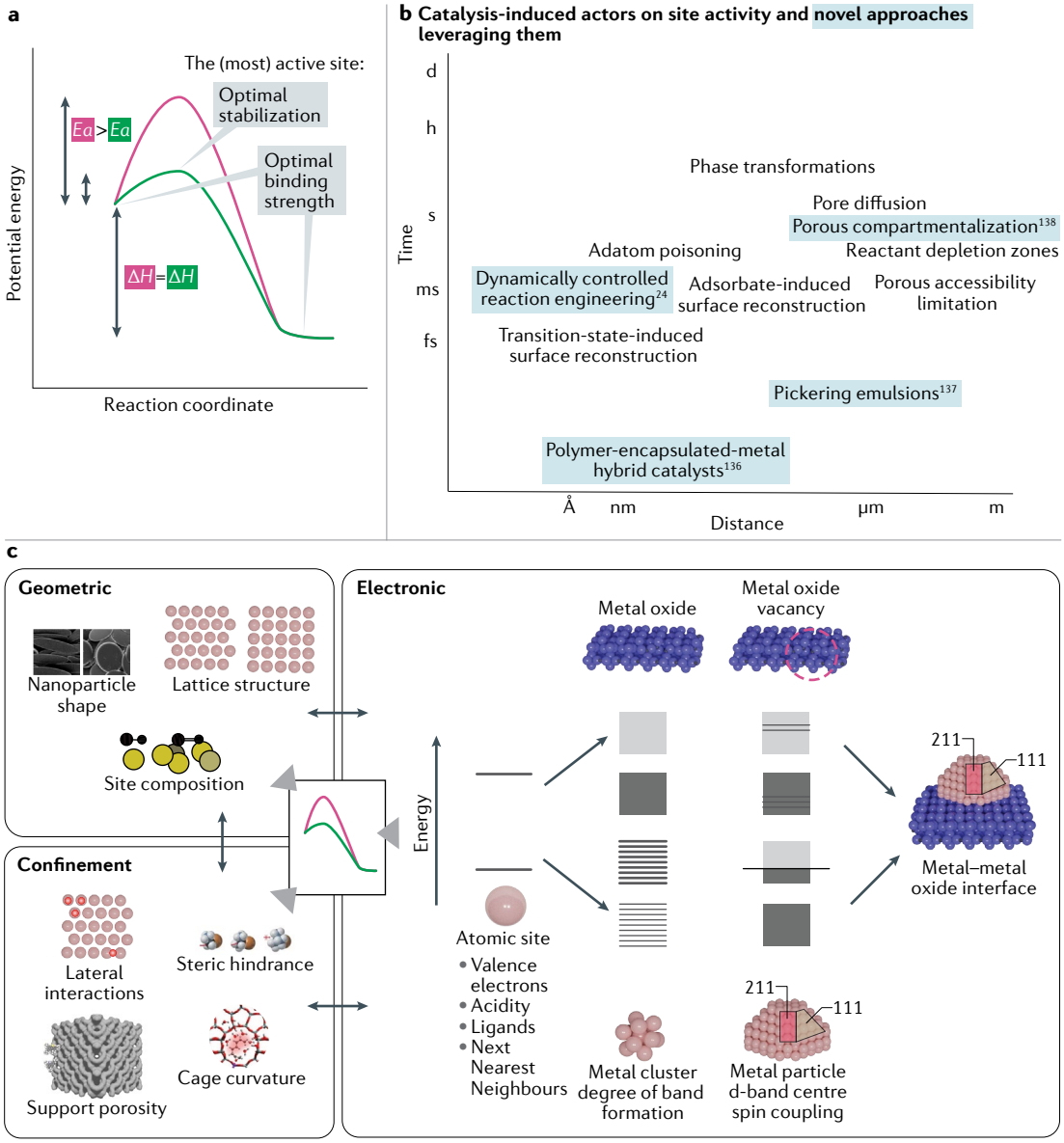

Fig. 1 | **Examining catalytic activity from an active site perspective. a** | Principles of catalysis, involving the kinetics, thermodynamics, as well as the role of the active site, including Sabatier's concept, and Pauling's transition state theory and how they relate to catalysis at the active site. **b** | Several factors that influence active site activity and their length scales and timescales are portrayed, as well as some novel approaches to increase site activity and their respective length scales and timescales[26,104,205,206]. **c** | Geometric, electronic and confinement effects are three correlated but separable parameters that heavily influence the activity of an active site.

Turnover number
In enzymology, the maximum number of chemical conversions of substrate molecule that a single catalytic site will execute for a given concentration. In organometallic catalysis, the number of moles of substrate that a mole of catalyst can convert before being deactivated.

Taylor ratio
The fraction of the catalyst surface that is catalytically active.

Surfaces reconstruct[25], while reactants and intermediates can be locally depleted[26] (FIG. 1b). To define an active site in heterogeneous catalysis is to understand these complexities and its dynamic variability in various reaction environments, be they liquid phase or gas phase, and as a function of reaction temperature and pressure. Hugh Stott Taylor (1890–1974) was one of the first to allude to this complexity and variability in active sites. He realized that the entire surface of a metal nanoparticle did not participate in a catalytic reaction but, rather, certain active centres. In doing so, he defined what is now termed the 'Taylor ratio'[27–29], which relates the fraction of active sites to the total exposed surface, and is, hence, always <1. Several excellent review articles and textbooks are available in the literature, which have helped us to highlight and explain catalyst complexity and variability in terms of surface reactivity[4,13,30–35].

Types of active sites

There are many different kinds of heterogeneous catalysts, and they can contain many different types of surfaces, and, hence, also active sites (TABLE 1). Brønsted acid (proton donating) and Lewis acid (electron withdrawing) are the sites that lead to catalytic activity in solid acid catalysts[1–4]. The formation or breaking of a covalent bond is often involved in these two types of catalysis, and these two types of active sites are intimately linked. Industrially, a prototypical example of the use of

Brønsted acid sites as the active phase is the fluid catalytic cracking (FCC) catalyst, which is currently used to convert a large fraction of heavy crude oil fractions into bulk chemicals, such as gasoline and propylene. These FCC catalysts contain zeolites, which, themselves, possess both Brønsted and Lewis acidity, but are then mixed in formulations with certain amounts of alumina or silica as binders, which can also have Lewis acidity (FIG. 2a). Furthermore, not all zeolites have the same T (tetrahedral) sites (the site where a tetravalent silicon atom is replaced by, for example, a trivalent aluminium atom), and T sites can vary both within a zeolite and as a function of process time (as a result of, for example, steaming). As the relative positions for Al substitution can differ, different Brønsted acid sites can exist. The same complexity holds for Lewis acid sites. BOX 1 goes into more detail on the complexity of (among others) the industrial FCC material as a prototypical example of a heterogeneous catalyst.

Metallocene polymerization catalysts are a typical example of catalysts believed to rely predominantly on Lewis acid active sites (although it must be noted that this is a somewhat simplistic definition and, in reality, the active sites are likely combinations of Lewis acidity and redox behaviour)[36–39]. Velthoen et al. recently studied the structures of a multitude of group 4 metallocenes (sandwich complexes of the metals with cyclopentadienyl-derived ligands), using density functional theory (DFT) and diffuse reflectance (DR) UV–vis spectroscopy[40]. By building a library of several different complexes, and simulating DR UV–vis spectra, their greatly convoluted, experimentally obtained spectra could be understood. They were, thereby, able to link the formation of $AlMe_2^+$ to the activity of the polymer catalysts. The active catalytic complex undergoes several activation steps in a complex scheme. Cl ligand abstraction by $AlMe_2^+$ eventually forms active (FIG. 2b) and dormant species, which once more react with $AlMe_2^+$ in a delicate balance between the active species and the polymeric form. Nevertheless, they also showed that the degree of activation of these catalysts is certainly not always 100% or even uniform. A showcase for this distribution in activity of sites is that the dispersity index of polymers is almost never 1. Another interesting notion about polymerization catalysts is that they greatly expand during catalysis, almost like pieces of popcorn popping, thereby, dynamically and increasingly limiting access to active sites[41,42].

The first evidence for the importance of basic active sites in zeolites was given by Yashima et al. for the alkylation of toluene with methanol[43]. It is suggested that these sites in zeolites are generally cationic sites of low coordination, and the population of these sites was inversely correlated with the Si/Al ratio. The Lebedev process to make butadiene from ethanol is an example of a catalyst with basic sites like those in, for example, SiO_2–MgO. These types of catalysts, nevertheless, almost always also contain Brønsted and Lewis acidity[44–48] (FIG. 2c). The Tishchenko process is another example of a reaction catalysed by a strong base, whereby ethyl acetate is formed by the esterification of acetic acid with ethanol catalysed by, for example, an alkoxide[44,49].

Redox sites are defined as those in which the valence state of the active site changes during the catalytic cycle. The formation of ionic bonds is often involved at the active site of this type of catalysis, but covalent bonds can also be formed[2]. An example of redox sites described in the literature are the Ni-alkyl species that create mobile active sites in SSZ-24 zeolite pores for an ethene oligomerization catalyst[50–53]. These sites are proposed to be isolated Ni^{2+} cations grafted on, for example, acidic silanol groups for the production of ethylene oligomers[50,54]. Another example of redox site formation is the formation of a multinuclear Cu site in the selective catalytic reduction of NO_x in a Cu-chabazite (CHA) zeolite[55–57]. In this example, Cu ions travel through the zeolite pores but experience electrostatic tethering, which limits their mobility. The nature of the active site of this reaction is under debate, and FIG. 2d shows one of the several proposed Cu nuclearities and conformations in this reaction[18]. This type of catalysis mainly occurs in metal–zeolite catalysis, in redox or atomically dispersed catalysis, such as is the case for olefin polymerization. It is interesting to note that these two examples both show that active sites themselves can be created, are dynamic and that their structures are a function of the exact reaction conditions that are applied to a catalyst material. A more recent study by Copéret and colleagues has reinvigorated the discussion of propylene epoxidation catalysts (TS-1), in which, rather than the single Ti atom sites that were the consensus for nearly 20 years, dimeric Ti atoms are now proposed to be responsible for the efficient industrial synthesis of propylene epoxide. Their results were obtained with a relatively novel methodology for these types of systems, using ^{17}O-labelled H_2O_2 for NMR. This has often been the trend; a new powerful analytical method often reveals a new feature or provides new insights, and this, in turn, leads to the proposal of a new active site[58].

The last type of catalytic activity discussed in TABLE 1 and FIG. 2 is that of a metal site. The distinction between a redox site (in, for example, atomically dispersed catalysis) and a metal site (in supported metal catalysis) is not necessarily absolute but made here based on predominantly single atom (ligand defect, redox site) versus

Table 1 | **Characterization of active sites by catalyst type and bonding, with an example of a chemical reaction**

Active site	Type of solid catalyst	Type of bonds involved	Chemical reaction example
Brønsted acid site	Solid acid	Covalent	Cracking of hydrocarbons, alkylation, methanol to olefins
Lewis acid site	Solid acid, atomically dispersed catalysis	Covalent	Olefin polymerization, cracking
Base site	Mixed metal oxides, hydrotalcite	Covalent	Lebedev process, Tishchenko reaction
Redox site	Atomically dispersed catalysis, clusters of atoms/ions, supported metal	Ionic, covalent	Selective catalytic reduction of NO_x with NH_3, selective oxidations
Metal site	Supported metal, atomically dispersed catalysis	Metal covalent hybrid	CO oxidation, (de)hydrogenation, Fischer–Tropsch synthesis

bulk metal properties (metal site). The chemical bond between an adsorbate and a catalytically active metal surface can be classified as a hybrid between a covalent and a metal bond[2]. In an active metal site, often, more than one metal atom participates to stabilize the transition state of the molecule that is to react[59]. This can be a cluster of atoms with specific geometric properties, as in the Fischer–Tropsch synthesis of hydrocarbons, where it is postulated that a B_5 site (a site where an incoming molecule incurs five contact metal atoms)[60] is believed to be the main active site for CO activation. But it can also be a site, for example, at the interface between a metal nanoparticle and its support[61,62]. A prototypical example of metal-based catalysis is the automotive exhaust catalyst[63–65], which consists of noble metals, such as Pt or Pd, which are present as metal nanoparticles and where, for example, carbon monoxide is oxidized to carbon dioxide (FIG. 2e). Although it is generally accepted that metallic Pt and Pd are the active phases, there are studies in which oxides of Pt and Pd are considered to be involved in the activation of small molecules, illustrating the complexity in discriminating between the different metal sites, the existence of metal oxides, as well as the interfacial structure between the support oxide, for example, an Al_2O_3 wash coat, and the metal sites[66–68] (FIG. 2e).

Influencing the activity of a site

If we compare Brønsted and Lewis acid catalysts, basic sites, redox site catalysis and metal catalysts (TABLE 1) among heterogeneous catalysts, many analogies affecting the types of active sites can be drawn between them, which helps us to unify important principles in catalysis. Because these types of catalysts have been studied in great detail over the past decades[12,69–73], some

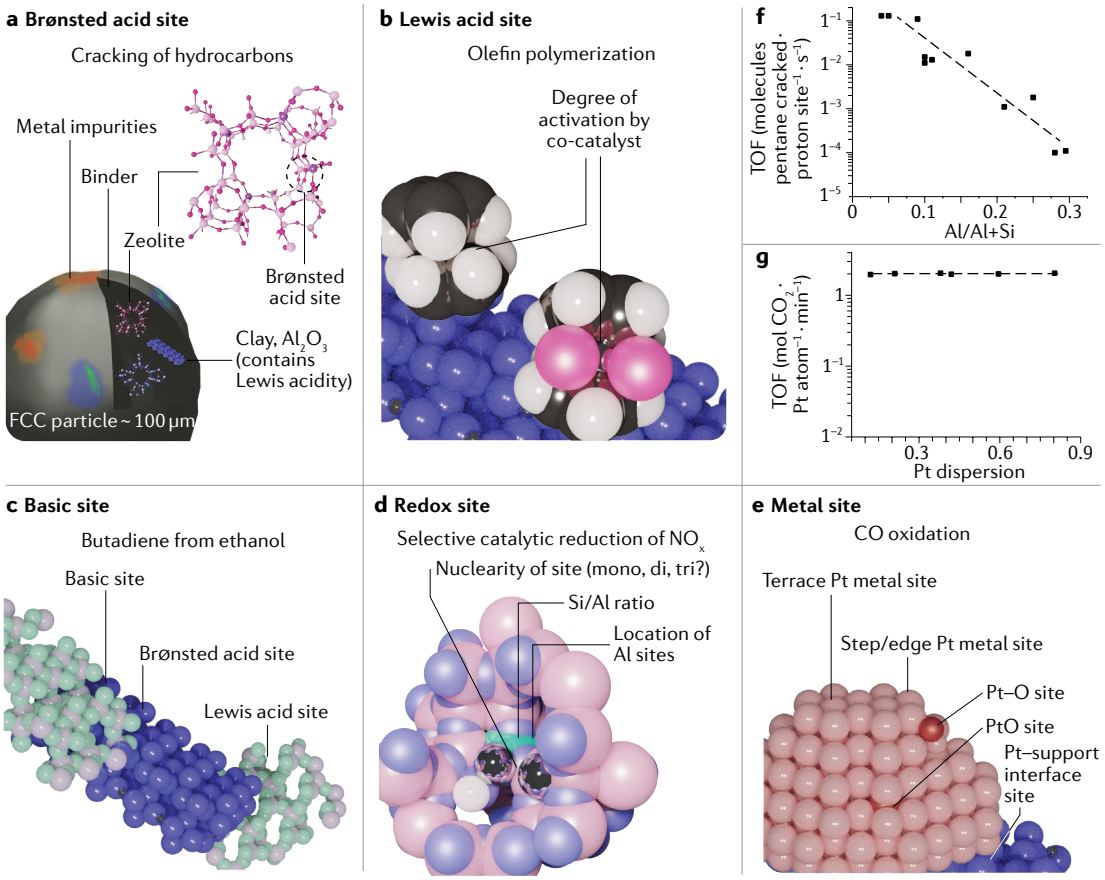

Fig. 2 | **Examples of catalysis arranged by type of active site. a** | Cracking of hydrocarbons in the fluid catalytic cracking (FCC) process, where the active site is a Brønsted acid site. Blue/green indicates Ni impurities, while orange indicates Fe impurities. **b** | Polymerization catalysts often need to be activated by an additive, a co-catalyst, yet, it is well understood that different degrees of activation occur throughout the catalyst particles. **c** | The Lebedev process for the formation of butadiene from ethanol proceeds over SiO_2–MgO catalysts, which generally possess both basicity and acidity. **d** | Selective catalytic reduction of NO_x typically occurs in a metal-substituted zeolite, of which the nuclearity of the active site is a topic of heavy debate, and is intimately related to the preparation procedure of the zeolite. **e** | CO oxidation is a typical reaction that occurs over a supported metallic nanoparticle catalyst (often Pt), yet, it is a matter of heavy debate whether the active site is Pt metal, O-bound Pt or PtO, or even Pt–support interface sites. **f**,**g** | Literature examples where the turnover frequency (TOF) is reported for reactions in parts **a** and **e**. The figure was created using data available in the original publications[207,208]. If one considers only the complexities highlighted in parts **a** and **e**, it already becomes clear that this potentially overlooks many important subtleties. Nevertheless, some interesting effects can be visualized with these plots, for example, the next nearest neighbour aluminium atom concept in part **f** or 'structure insensitivity' in part **g**. Dotted lines are linear fits to the data, drawn as a guide to the eye.

Box 1 | **The complexity of the industrial catalyst**

A fluid catalytic cracking (FCC) catalyst particle is an excellent illustrative example for the complexity of defining the 'active site' in real, industrially applied heterogeneous catalysts. Brønsted acidity is often credited for the observed catalytic activity of this crude oil cracking process. In reality, the cracking reaction, and of side reactions, are much more complex. Zeolites indeed donate protons to alkenes, forming a carbenium ion (these are also formed, to a certain extent, by thermal cracking of the alkane mixture). Cracking occurs by β-scission of this carbenium, which transfers a proton (or abstracts a hydride) to form a new carbenium ion[22] (see the figure, part **a**). If this continuous transfer of carbenium ions occurs at a faster rate than the amount of proton donations from the zeolite, what is the actual catalyst and what would be the turnover frequency? To report turnover frequencies (FIG. 2f) for such hugely complex systems requires the assumption that the Si/Al ratio is a direct measure for the amount of active (proton) sites, and this is quite obviously far from reality. Under the strictest definition, the zeolite here is merely a co-catalyst (the same is true for the methanol-to-olefins process, where the actual catalysis takes place on the 'hydrocarbon pool', the formation of which is facilitated by the zeolite)[142,143]. This is just the cracking process alone, whereas the ageing of real industrial FCC catalysts leads to increasing amounts of metal poisons, such as Ni and Fe, to form a shell around the FCC particle (see the particles measured by X-ray microscopy depicted in parts **b** and **c** of the figure with 3D speciation of metal deposits affecting pore accessibility and see also the average Fe concentration and porosity change due to Fe deposits as measured by X-ray nanotomography[70]. These metals can catalyse hydrogenation and dehydrogenation reactions, but they can also block access to the inner parts of the FCC particles. Part **d** of the figure describes a spent FCC particle indicating blockage by metals (La, Fe and Ni), but also by coke formation both on the surface and within the FCC catalyst particle in grey and magenta, respectively. The different phases in FCC formulations (which are responsible both for the desired cracking reactions and also for side reactions with Ni and Fe), the matrix (LAS), binder (LAS), zeolite (BAS, redox) and, finally, metals are schematically shown in FIG. 2a. Taking this all into account, it becomes clear that even this prototypical example of a well-defined heterogeneous catalytic active site as a Brønsted acid site is, in reality, far, far more complex, and ascribing a turnover frequency value for the active site is very difficult.

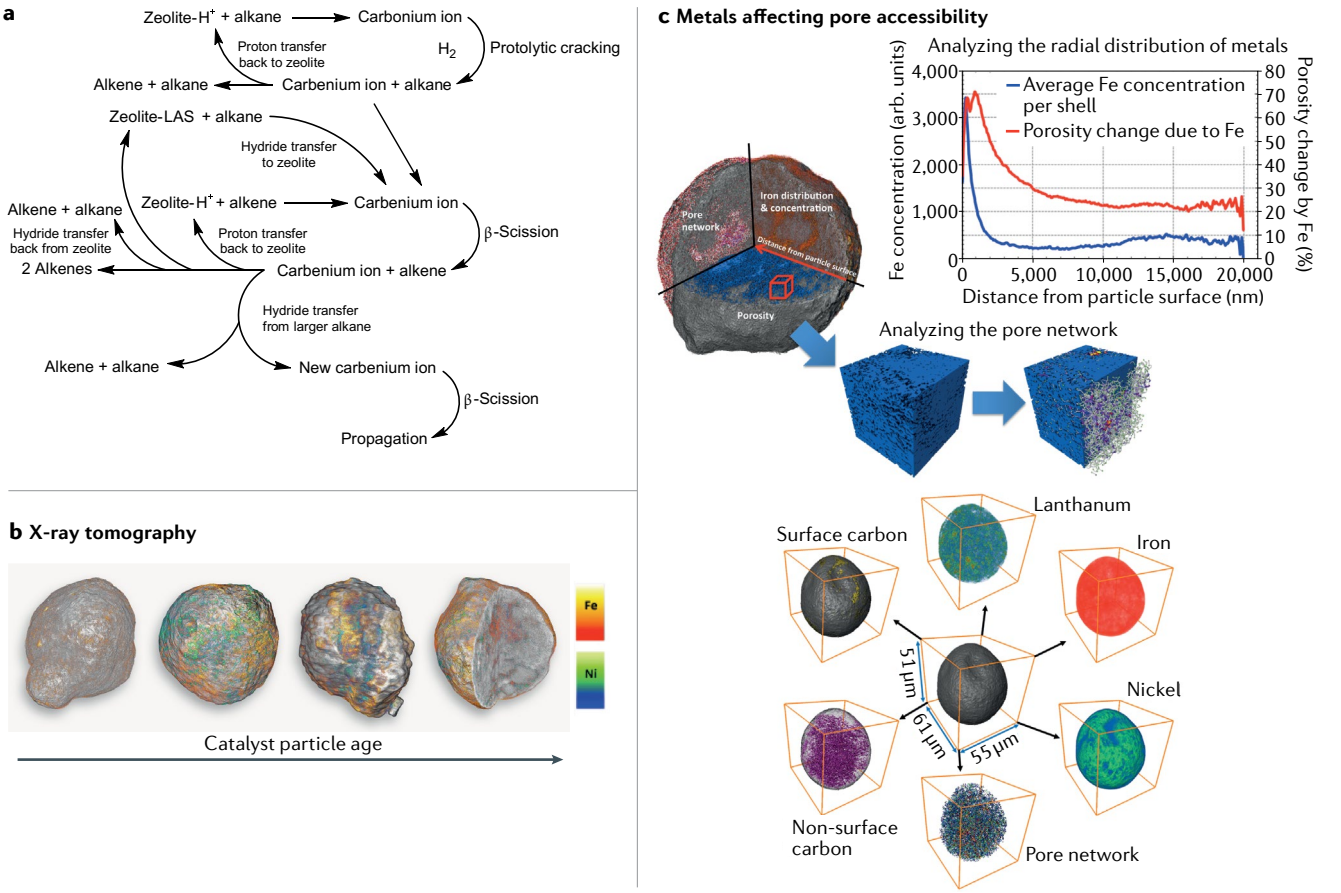

Part **a** is reprinted with permission from REF.[22], RSC. Part **b** is adapted with permission from REF.[70], AAAS. Part **c** is adapted with permission from REF.[211], CC BY 4.0 (https://creativecommons.org/licenses/by/4.0/).

fundamental comparisons can be made with respect to the active site in heterogeneous catalysts. FIGURE 1c schematically shows an overview and examples of the different parameters influencing the activity of the different types of active sites discussed.

Geometric effects. It is important to note that the active site can technically be located at a single atom for supported metal nanoparticles, for solid acids and for atomically dispersed catalysts. This final type of active sites are often also termed single-atom catalysts, a term that is somewhat under scrutiny, but refers to heterogeneous catalysts with atomically dispersed metal atoms[74]. Nevertheless, the workings of an active site would be very different were it not surrounded by other atoms; the same 'active' atomic site may even be completely inactive, depending on the geometrical environment[17–20]. This fact is externalized in different ways for the different classes

Box 2 | **The concept of structure sensitivity**

An interesting, empirically observed fundamental phenomenon in catalysis is called structure sensitivity, which is best defined as "not all atoms in a catalytic nanoparticle having the same catalytic activity"[75,110,212]. This concept is classified by taking a measure for the available surface and dividing the activity by this (leading to a turnover frequency (TOF)), and then plotting this TOF against particle size. Building on observations from many others[171,172], Michel Boudart (1924–2012) noted that reactions can be either 'facile' (a TOF independent of nanoparticle size, or structure insensitive) or 'demanding' (a TOF dependent on nanoparticle size, or structure sensitive)[109]. This is now commonly explained by the preferential cleavage of σ-bonds at highly uncoordinated atoms and preferential cleavage of π-bonds at defect sites. See also part **a** of the figure displaying the calculated percentage of neighbour atoms in Wulff-constructed nanoparticles of different sizes, where one can see that a small nanoparticle has much more surface relative to a large one, and, of this surface, much more is under-coordinated (steps or edges) rather than highly coordinated (terraces). Part **b** of the figure shows the trends in TOF typically observed for these types of activities: an exponential decrease in activity with increasing particle size for σ-type sensitivity, an optimal particle size for π-type sensitivity and a flat line for structure-insensitive behaviour[31,109,110,213]. These site preferences can lead to different types of empirically observed structure–sensitivity trends. The figure also summarizes some literature data for different classes of structure sensitivity, all plotted on the same scale. Reactions are shown in which the activation of a σ-bond (part **c**, steam methane reforming, $CH_4 + H_2O \rightarrow CO + 3H_2$)[214–221] or a π-bond (part **d**, carbon dioxide methanation, $CO_2 + 4H_2 \rightarrow CH_4 + 2H_2O$)[12,222–224] is believed to be rate limiting, and for a classical structure-insensitive reaction, where the rate-determining step is believed to be the recombination of an adsorbed alkyl (part **e**, ethene hydrogenation, $C_2H_4 + H_2 \rightarrow C_2H_6$)[225–227]. There have been numerous reports of an absence of a structural dependence in the rate of ethene hydrogenation to ethane over single-crystal facets[225,226,228]. Nevertheless, when one examines the profiles observed in part **e** and compares them to part **b**, the structure insensitivity of ethene hydrogenation is not so obvious. Thus, the only figure that resembles the class of structure sensitivity that it is often assigned to is that shown in part **d**, π-bond activation. These observations show that there is still much to be explained, and that the TOF is not a uniform way to relate the activity in different studies, as it is based on the general (and clearly erroneous) assumption that all exposed surface area is (equally) active. A more comprehensive explanation, and details of these descriptions, are given in the Supporting Information. The way we describe kinetics of catalytic reactions in general is also still based on the adsorption isotherm of Langmuir (1915) and the kinetic formalism of Hinshelwood (1927), based on ideal surfaces with equivalent adsorption sites and adsorbates that are randomly mixed and do not interact. We are becoming more and more aware that this picture is far more complex.

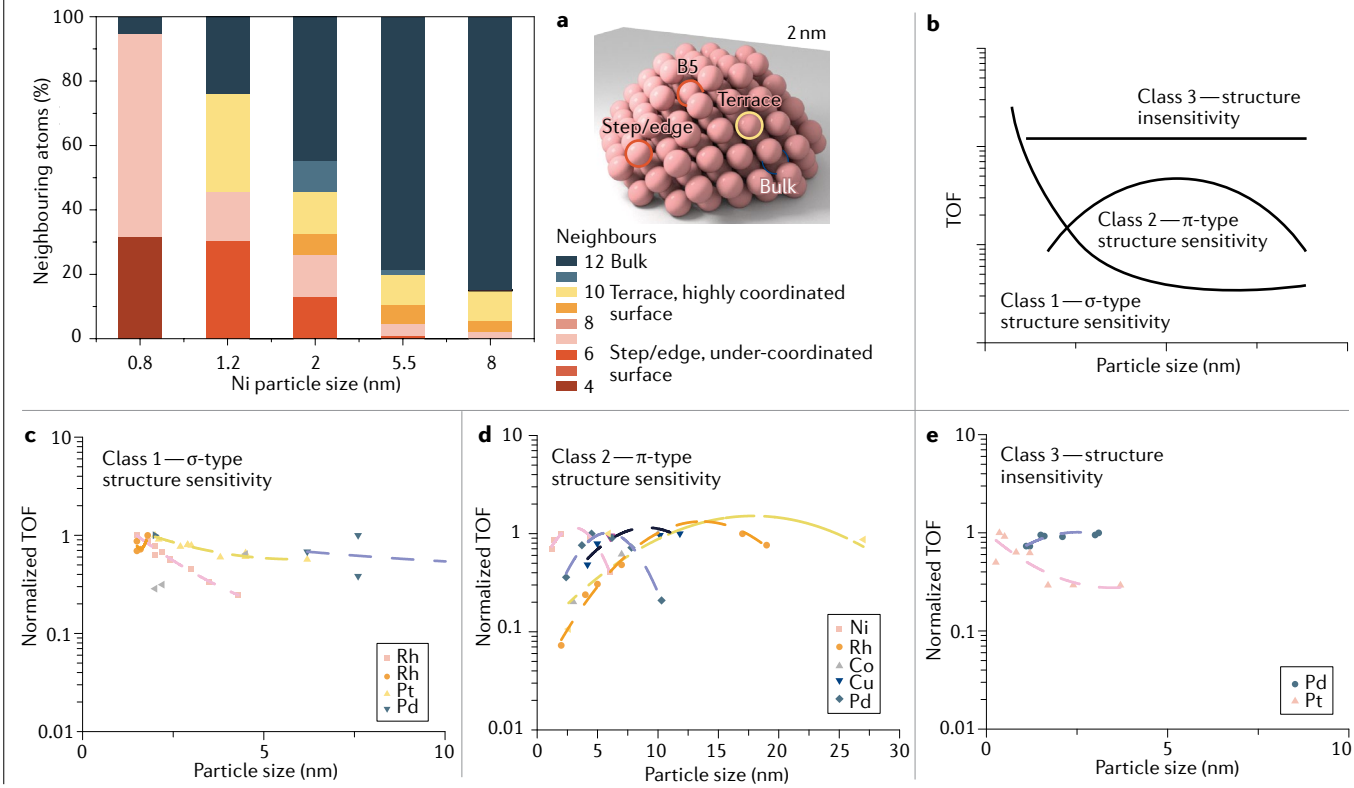

of catalysts as, inherently, different types of bonds and length scales — and, thus, geometries — are involved in the different classes. Geometric and electronic effects on the active site are closely correlated, but can be separated based on Brønsted–Evans–Polanyi relationships[13] (BOX 2).

For metal catalysts, different facets can be exposed by different particle sizes, which can be seen in FIGS 1c,3a. Michel Che (1941–2019) and coworker reviewed the influence of metal nanoparticle size on the catalytic properties of supported metals[75]. Leland Cratty (1930–2019) and Andrew Granato (1926–2015) proposed that 'dislocations' may actually be the active sites in supported metal catalysts[76]. Many experiments have been performed to bolster this hypothesis and many of the results have been interpreted assuming lattice imperfections as active sites[77–79]. Nowadays, it is widely accepted that highly under-coordinated sites, such as steps or kinks, similar to Cratty and Granato's 'dislocations', can have much higher catalytic activity than other sites. The reason for this is, in part, attributed

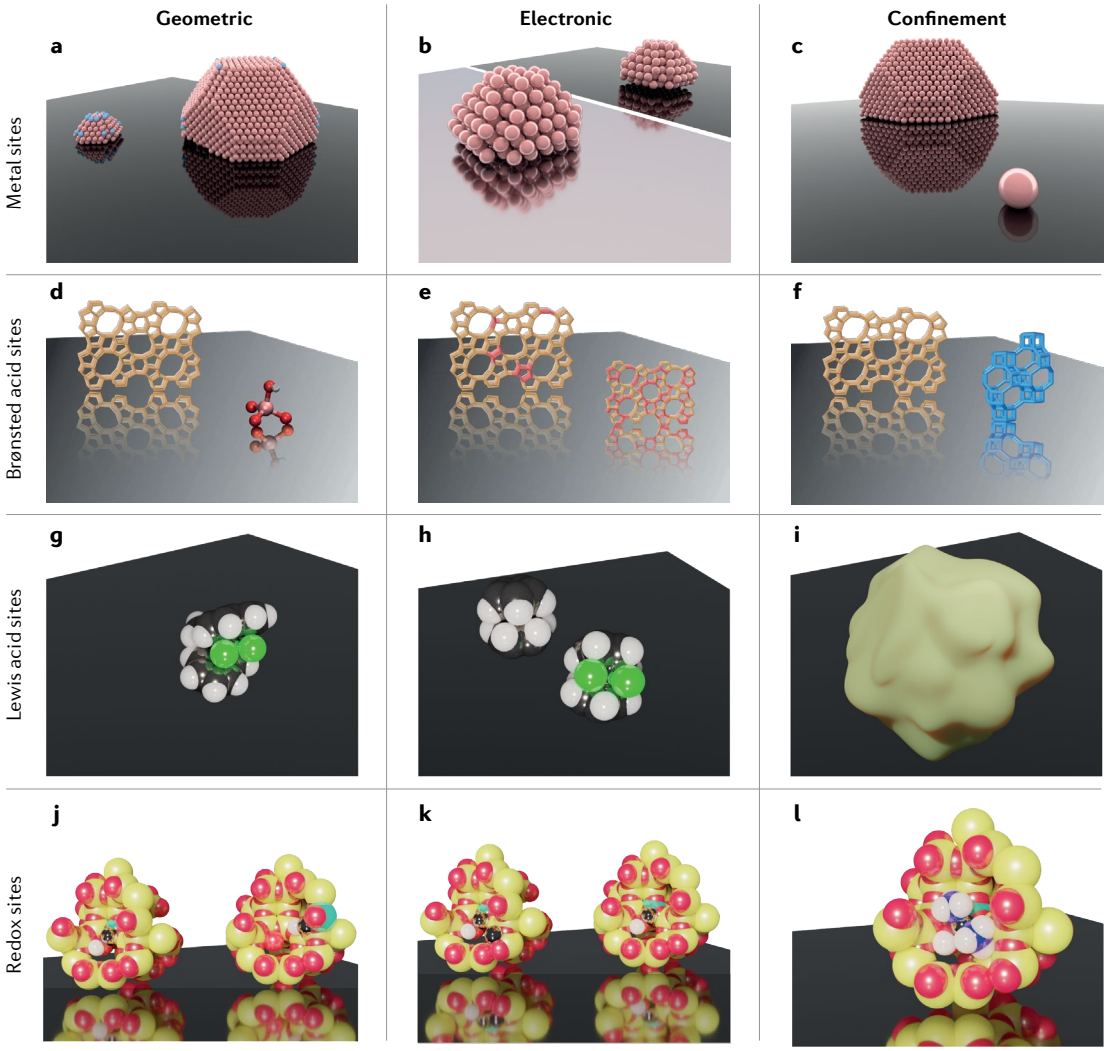

Fig. 3 | **Geometric, electronic and confinement effects combine to dominate the activity of an active site in heterogeneous catalysis.** These three effects, geometric, electronic and confinement, are illustrated for each type of catalyst considered: metals (parts **a**–**c**), Brønsted acids (parts **d**–**f**), Lewis acids (parts **g**–**i**) and redox (parts **j**–**l**). Geometry affects the configuration of sites within a metal nanoparticle. Active sites may be known to exist at, for example, the edge of a crystal facet. The fraction of a particular type of metal site is then heavily dependent on metal particle size; there are relatively more blue sites on a smaller nanoparticle than a large one (part **a**). Electronic effects can be seen to result from different supports (for example, a reducible support like TiO_2 versus a non-reducible one like SiO_2). These effects are increasingly important as the size of nanoparticles is reduced (part **b**). Confinement, for example, in terms of intraparticle distance or the distance of a given site to any other (part **c**). For solid acid catalysts, examples are: the strength of the acidity of a Brønsted acid site (part **d**), which is dependent on the geometry of the zeolite structure, as the same atomic composition making a Brønsted acid site (shown) can have completely different acid strength, depending on, for example, the curvature of the given zeolite ring structure; the Si/Al ratio in a zeolite is an electronic influence on the acidity of acid sites in a zeolite (part **e**), for example, through the next nearest neighbours concept. Shown are two identical zeolite structures, with differing Si/Al (yellow/red) ratios); the confinement of an acid site (part **f**), such as a large cage or pore compared with a small cage or pore, influences the relative strength of that acid site on a reactant; a Mobil Five and a chabazite (CHA) type zeolite have differing cage and pore confinement. For 'atomically dispersed' catalysts, the examples are: in metallocenes (part **g**), the steric properties of the size of ligands is a determining factor in selectivity and activity by influencing site accessibility geometrically; furthermore, the electronic properties of ligands can also influence activity and selectivity (part **h**), for example, in zirconocene versus zirconocene dichloride shown here. For visual clarity reasons, the methylaluminoxane that is used to activate the metallocene complex by removal of a Cl (indicated in green) ligand[40] is not shown, the actual active site in metallocene catalysts only arises after this activation but it is, nevertheless, influenced, also in its active state, by the described phenomena; the 'popcorn-like' structure of growing polymer particles increasingly confines and eventually deactivates the active sites of polymer catalysts (part **i**). For redox sites, the examples are: the location of the Al substitution influences the geometry and type of Brønsted acid site in a zeolite (part **j**) (shown are two green Al atoms in a CHA cage with yellow Si and red O atoms); the nuclearity (part **k**) (shown mono, di) of the metal site in CHA; and the confinement of the Mobil Five network with a single copper atom (part **l**) strongly influences the activity of NO_x selective catalytic reduction[57].

to their localized geometry, which is the geometric structure of their localized electron density (such as the different localization of orbitals protruding from a site).

For a zeolite, geometry can be thought of in terms of the reactivity of a single Si–O(H)–Al Brønsted acid site or one that is built into a specific position within a ring of a zeolite[80,81] (FIG. 3d). The reactivity of these sites will be different depending on, for example, zeolite pore size (curvature/lattice strain), even though they can be built from the same fundamental constituents[82,83]. The same holds for redox sites in zeolites.

For Lewis acid catalysts, such as metallocenes, the steric properties, or the geometry, of ligands is a determining factor in selectivity and activity[2,27]. This is illustrated in FIG. 3g, where a non-activated metallocene is shown (for visual simplicity). In reality, methylaluminoxane is added to activate this type of polymerization catalyst by withdrawing a Cl ligand, thus, creating the active site — a Zr^{+} ion sandwiched between two cyclopentadienyl rings that help to propagate polymerization of ethylene with specific selectivity[40]. The steric properties of the ligands in such olefin polymerization catalysts are highly important steering factors in the desired properties of the plastics that are produced by them. van Bokhoven and colleagues recently showed that octahedrally coordinated aluminium is the precursor of a Lewis acid site in mordenite, and that the formation of such a site is accompanied by a reduction in Brønsted acidity[84,85]. The local geometry of these sites is extremely important, because it determines whether a site has Brønsted (tetrahedral) or Lewis acidity[84]. FIGURE 3j shows a CHA zeolite with differently located Al substitutions, which can make a large difference in the reactivity of the Brønsted acid site following from it.

Electronic effects. Geometric and electronic properties are inherently related, as mentioned above and further discussed in BOX 2. Nevertheless, the structure–activity dependence (for metal catalysis) has frequently been shown to be divisible into these two fundamental constituents. This method of thinking can, arguably, be extrapolated also to Brønsted and Lewis acids and redox catalysts, noting that electronic effects are, in fact, the most important determining factor in catalytic site activity, even going so far as to say that, without an electronic effect, there would be no catalysis. This observation forms the basis for Sabatier's principle, which is an elegant explanation of the effect of electronic structure on catalysis: Sabatier plotted the binding energy of an adsorbate against the reaction speed; the resulting 'volcano plots' indicate that the catalysis is most effective when the electronic interaction between the adsorbate and the substrate is neither too strong nor too weak[12–15].

Now, approximately a century later, we are still trying to understand the subtleties of this concept. FIGURE 1c illustrates that the position, separation, degree of coupling and so forth of energy levels reveals a great deal about an active site. For example, the 'scaling relations' introduced by Nørskov and colleagues for catalysis on metals[86,87], which relates the position of the d-band of a metal to adsorption energies of reactants, and adsorption energies to activation energy barriers, have been extremely successful in determining activity parameters and related trends in catalytic reactions[87]. These scaling relationships are important for two main reasons; first, they allow the determination of reaction energetics with fewer calculations, allowing for rapid screening by making a general assumption that the properties of (combinations of) metals or surfaces for a given catalytic reaction can be compared based on their electronic energy levels[88]. Second, the scaling relations allow researchers to establish and highlight the gap between current experimental reality and theoretical possibility, giving experimentalists an end goal for catalyst design improvement[88–90]. However, refinements can and must still be made, such as taking into account the importance of spin coupling to magnetic transition metal surfaces[91].

Electronic effects are not limited to the composition of the active site but are also important for its surroundings. That is, for example, why a support material is used for supported metal nanoparticles (FIGS 1c,3b), the ratio of silica to alumina used in a zeolite formulation (FIG. 3e), which ligands are used in an metallocene-catalysed olefin polymerization (FIG. 3h), or the nuclearity of a redox site (FIG. 3k) are important. The smaller a metal nanoparticle becomes, the more significant the effect of a support can become not only as a result of increased particle–support interface but also due to the effect on the band structure of the metal nanoparticle[6,92,93] (FIG. 1c).

Confinement effects. The third parameter that can greatly influence the active site and, thus, catalytic activity, is confinement[82,83,94–97] (FIG. 3c,f,i). Regardless of whether the active binding site consists of a single bond or a single site, its confinement is extremely important. This parameter is best explained using solid acid catalysts as an example. Fraissard was (most probably) the first to pose the question: "Why are zeolites so much more active than amorphous silica–alumina?", the answer being that "the molecule absorbed in a zeolite is subjected to an 'apparent pressure' about 100 times greater than the pressure upon a molecule in contact with a planar surface")[98]. Later, Éric Derouane (1944–2008) and colleagues were the first to explain that the activity and selectivity of different zeolites in the cracking of n-pentane is related to the pore size of the zeolite under study[82,94]. In fact, they showed that it is not the acidity of different zeolites that results in different turnover frequency (TOF) for different zeolites but, rather, the confinement of the reactant in the zeolite. That is, in two fully comparable active sites, the TOF (corrected for the number of acid sites) is dependent linearly on the pore size[97]. This effect was explained by describing the van der Waals energy of a spherical molecule as exponentially dependent on the ratio between the van der Waals radius of that molecule and the micropore diameter[83]. Hence, importantly, acidity in zeolites should never be listed without consideration (and discussion) of the effect of confinement[82,94–97,99]. Other groups like those of Iglesia and Lercher continued in this line of research[100,101].

For Lewis acid sites, FIG. 3i shows a polymerized catalyst particle. Active sites are positioned in a silica matrix and are surrounded by a growing polymer chain. This growth breaks the particle open and frees new

active sites for polymerization. The changing morphology of the growing polymer particles has a significant impact on the rate of mass and energy transport, and, as such, on the polymerization rate, comonomer incorporation and the molecular weight distribution[102]. The possibility to control the final particle morphology by manipulating the catalyst and the support properties, as well as the reaction conditions, is of great interest for both academia and industry.

In supported metal catalysts, confinement can be defined as the influence of external activity on an active site. It is increasingly recognized that microenvironments are equally as important as the active site, a realization that is rooted in our understanding of nature's fully optimized catalysts, enzymes[103]. Cargnello et al. were recently able to demonstrate the validity of this concept for a Pd-catalysed CO oxidation using supported metal heterogeneous catalysis. The metal nanocrystals were encapsulated in microporous polymer layers[104] by separately preparing the Pd nanocrystals and microporous polymer material, and subsequently impregnating by dissolving both in hexanes. It was found that the polymer-encapsulated catalysts consistently showed higher TOF, by as much as an order of magnitude. The authors explain this observation by invoking a confinement effect, bringing the CO and Pd into close proximity prior to reaction and reducing the entropic penalty associated with formation of the reaction transition state. The polymer layers apparently stabilize the $CO_{(2)}$ intermediate through Lewis interaction of the species with nitrogen lone pairs on the amino groups present on the polymer layers. Somorjai suggested that enzyme catalysis and homogeneous catalysis are linked by two important properties of heterogeneous catalysis[34]. The first is the importance of under-coordinated sites for the making and breaking of bonds (the key concept in homogeneous catalysis) and the second being the influence that more complex structures such as overlayers, confinement and other environments have on more complex reaction pathways (such as consecutive elementary reaction steps). It is just such interactions that were observed by Cargnello et al.[104,105], and what the scaling relations described by Nørskov and colleagues point to[86]: tuning the microenvironment of catalysts makes them increasingly resemble enzyme-like active sites. Finally, FIG. 3| shows the confinement effect of zeolite framework type MFI (versus, for example, CHA) network with a single copper atom, which strongly influences the activity of NO_x selective catalytic reduction.

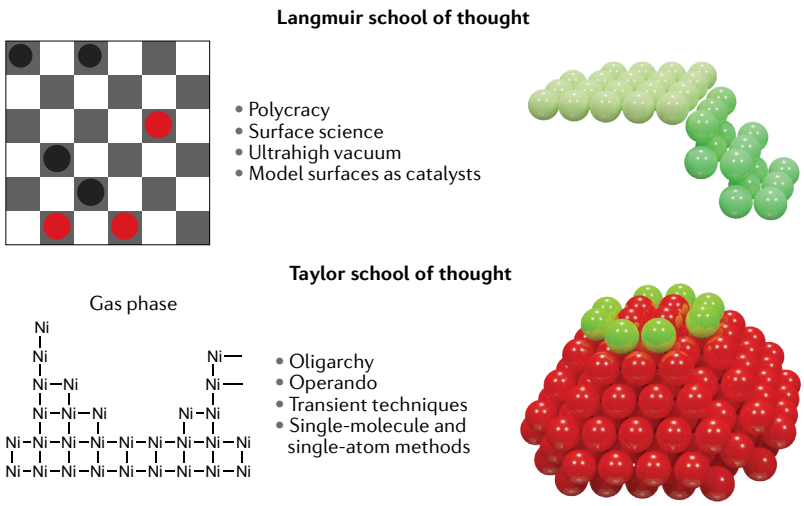

Fig. 4 | **The differences between the Langmuir and Taylor schools of thought.** Langmuir simplified the consideration of reactions at surfaces by considering them only in two dimensions, like a chequerboard. With this assumption, certain facets can be more or less active than others. The Taylor school of thought is a more 3D view, recognizing that there is crystalline anisotropy. His view is that there are some sites that are active (green) and some that are not (red), which make up the Taylor ratio.

The complexity of the active site

It is obvious that active sites in heterogeneous catalysis are extraordinarily complex (BOX 1). To understand such complex systems, we, therefore, as scientists, attempt to simplify them, make new predictions on that basis and see if they hold up under experimental conditions. Throughout the history of research focused on identifying and understanding the active site in heterogeneous catalysis, there are two main schools of thought. First, the Irving Langmuir (1881–1957) school of thought and, second, the Hugh Stott Taylor (1890–1974) school of thought. Langmuir's isotherm, and much of his work on surfaces, assumes a continuous monolayer of adsorbate molecules surrounding a homogeneous solid surface. "In order to simplify our theoretical consideration of reactions at surfaces, let us confine our attention to reactions on plane surfaces. If the principles in this case are well understood, it should then be possible to extend the theory to the case of porous bodies. In general, we should look upon the surface as consisting of a checkerboard…"[106]. The Langmuir school of thought was the main driver of surface science. It does not merely suggest, but relies upon, a 'polycracy' of equivalent surface sites (FIGS 4,5). On the other hand, the Taylor school of thought (FIGS 4,6) includes a higher degree of complexity and recognizes that surfaces are influenced by crystalline anisotropy, surface defects and various surface compositions. His active sites are 'oligarchs'; only a few exist, but they, nevertheless, dominate the catalytic activity, the rest of the surface being covered with spectator species. These two important schools of thought, while clearly differing, yet, not necessarily opposing, allow us, as the scientific community, to group together much of the technical developments, as well as our ever-increasing understanding of the active site. In what follows, we will discuss both schools of thought, concluding that neither display a complete picture of the complexity, after which we discuss our view on what is necessary for further development of concepts in catalysis.

Langmuir school of thought. Chemisorption has long been a staple tool for catalyst understanding. Michel Boudart, a PhD student of Taylor, and lifelong friend of Pauling[107,108], was heavily interested in measuring dispersion via chemisorption techniques and, thus, deducing the available surface exposed to a given probe (most often H_2 or CO), generalizing the measured exposed surface as active sites[109]. It is worth noting, of

course, that different reactants or intermediates may be adsorbed at different sites. Nevertheless, Taylor recognized that this value of exposed surface sites 'N' might only represent an an average and that not all sites would necessarily be active (or even active at all times)[110]. For many decades following the 1920s, kinetic

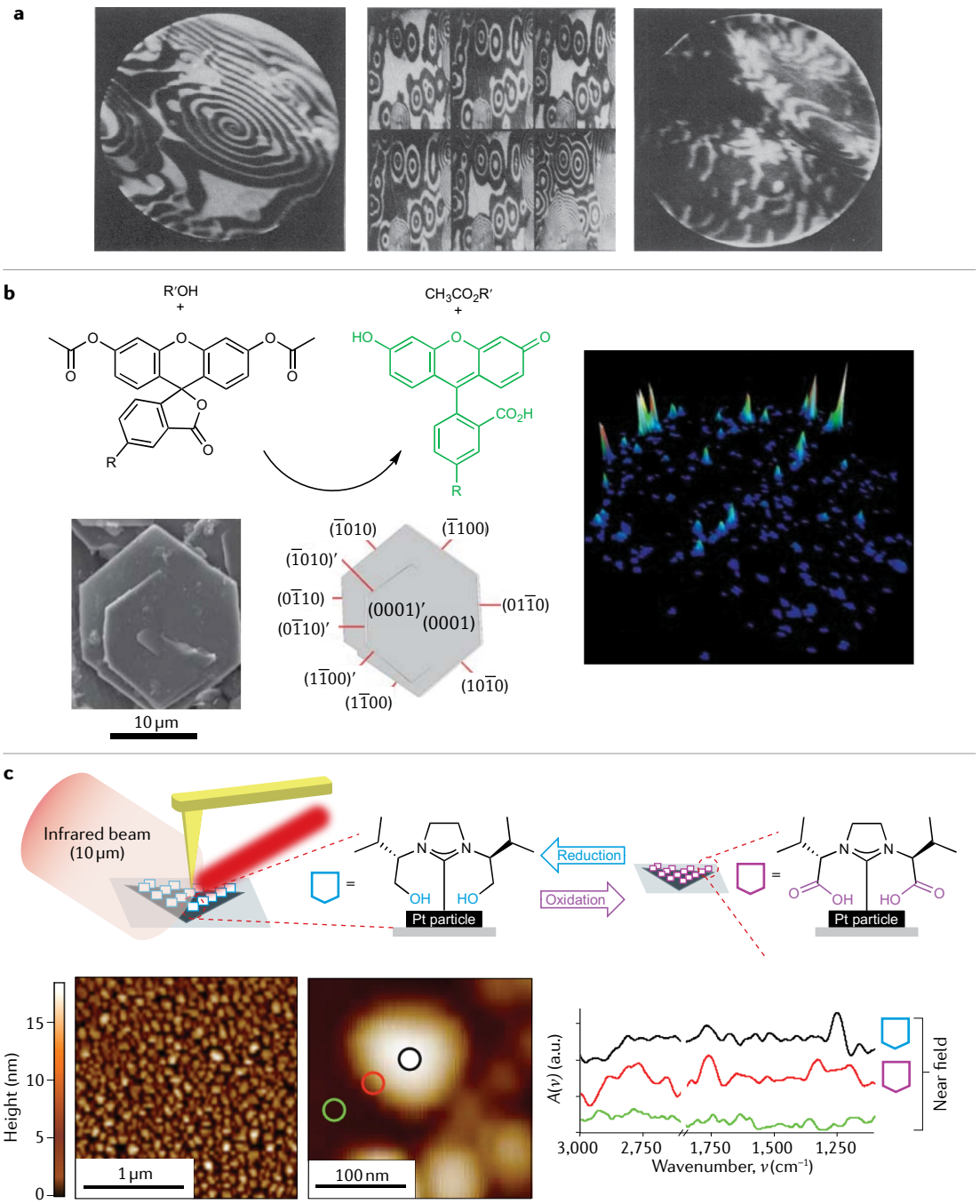

Fig. 5 | **Examples in support of the Langmuir school of thought. a** | Spiral wave patterns induced by CO (bright) and O (dark) on Pt(110) single-crystal facets as imaged by photoemission electron microscopy: rapid and irregular changing patterns caused by oscillatory surface kinetics and chemical turbulence. **b** | Gibbsite-type stacked sheets of Li^{+}-Al^{3+} layered double hydroxide were studied by wide-field microscopy, using the fluorogenic probe 5-carboxyfluorescein diacetate, which becomes emissive upon catalytic hydrolysis in water-containing media or upon catalytic transesterification. It was found that ester hydrolysis proceeds on the lateral {1010} crystal faces, while transesterification occurs on the entire outer crystal surface. **c** | The reduction and oxidation of N-heterocyclic carbenes was studied on Pt nanoparticles of approximately 100 nm in size by synchrotron-radiation-based infrared nanospectroscopy, with a spatial resolution of approximately 25 nm. It was directly shown that the sides of these nanoparticles, containing more stepped facets, were more active in the oxidation and reduction of chemically active groups on the N-heterocyclic carbenes than the flat tops of the Pt particles. Part **a** is reprinted with permission from REF.[25], AAAS. Part **b** is adapted from REF.[146], Springer Nature Limited. Part **c** is adapted from REF.[148], Springer Nature Limited.

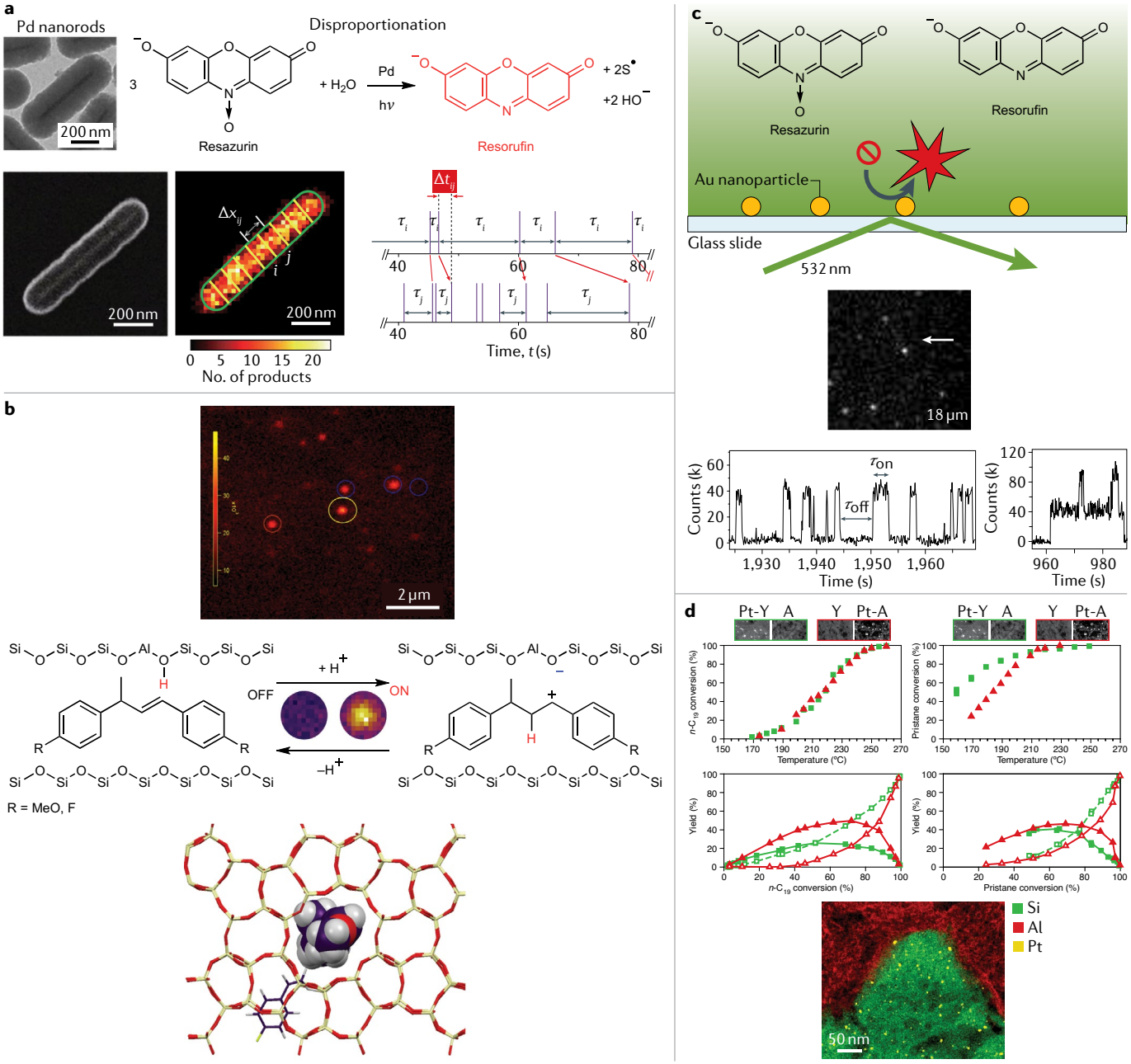

Fig. 6 | **Literature examples illustrating the complexity and diversity of the active site along the Taylor school of thought. a** | Scanning electron microscope image of a Pd nanorod (top) and a SiO_2-coated Pd nanorod (bottom), alongside a 2D histogram in which >6,000 fluorescent product molecules are binned in 25 × 25-nm² sections and mapped onto an outline of the particle taken from the scanning electron microscope image. The nanorod is divided into segments and the graph indicates catalytic event sequences from segments *i* and *j* in time *t* (s), with vertical lines indicating theformation of product and horizontal arrows showing the times between subsequent events. **b** | Probing the accessibility of zeolite H-ZSM-5 crystals with wide-field fluorescence micrographs of the Brønsted-acid-catalysed oligomerization of 4-methoxystyrene at different molar concentrations in heptane. **c** | Single-turnover detection of single-Au-nanoparticle catalysis of resazurin reduction, showing segments of the fluorescence trajectories (reaction events) from a fluorescence spot. At the bottom, multilevel events can be seen, which directly reflect the multitude of catalytic sites that can undertake catalysis in parallel, or docking sites, where products remain bound to the Au nanoparticle surface before dissociation. **d** | The impact of nanoscale intimacy on hydrocracking activity and selectivity of Pt catalysts deposited on either zeolite Y or the alumina component of Y/Z extrudates. At the bottom is a high-angle annular dark-field scanning transmission electron microscopy image showing the Pt dispersion exclusively on the zeolite. Part **a** is reprinted from REF.[149], Springer Nature Limited. Part **b** is reprinted with permission from REF.[209], ACS and REF.[210], Wiley. Part **c** is reprinted from REF.[166], Springer Nature Limited. Part **d** is reprinted from REF.[168], Springer Nature Limited.

analysis following Langmuir's adsorption isotherms was the major tool to understand catalytic activity. Developments in spectroscopy changed that and made it possible to study the relationships between structure and performance, thus, following more closely the Taylor school of thought. So far as we are aware, the application of spectroscopy in catalysis commenced with seminal publications from Robert P. Eischens (1920–2010)[111–113].

In situ spectroscopy
In situ spectroscopy entails spectroscopic investigation at one or more catalytic conditions (T, p, reactants).

He was most likely the first to perform in situ spectroscopy by building a cell consisting of two CaF_2 discs and a Pyrex tube to measure the infrared spectra of heterogeneous catalysts. The CaF_2 windows were coated with catalyst film, after which the device was placed in a furnace, where it reacted with molecules. The cell with the catalyst material and the adsorbed molecules was then transferred to a spectrometer.

Nevertheless, an overwhelming majority of studies contributing to our fundamental understanding in the literature have simplified in similar ways, following the Langmuir school of thought and assuming equivalent and well-defined active sites, for example, by using single-crystal facets, often under ultrahigh-vacuum conditions; this approach is termed surface science[105,114–121]. Surface science approaches in model systems have yielded many of the important insights on which we currently build our understanding. In recent decades, however, it has also become apparent that adsorbates and surfaces have completely different physical parameters, such as surface stability, mobility of species, surface coverage and surface energies, at the relevant conditions of pressure and temperature[105,122,123]. Several surface science groups around the world are attempting to close this gap by performing their experiments under less than high-vacuum conditions, approaching 'ambient' pressures, for example, in near-ambient pressure X-ray photoelectron spectroscopy[123–125]. Many of these approaches, however, still make use of model surfaces rather than the nanoparticles that are used in real-life applications, and these measurements are generally static. When a static measurement is performed on a surface that is in chemical and physical equilibrium, much information is lost as to how this equilibrium was reached. That is, for a given reaction intermediate to cover a surface, often, several sequential elementary reaction steps have occurred at the timescale of milliseconds to seconds, each of which has an effect on the surface and on the subsequent steps[30,31].

Nevertheless, to discuss the development of techniques to determine active sites in catalysis, one must discuss developments in surface science, which culminated in the award of the Nobel Prize in Chemistry for Gerhard Ertl in 2007 for the contributions of surface science to the field of catalysis[115]. Ertl's work shows, for example, that there are islands of adsorbed molecules (molecular adducts) and/or surface atoms (originating from dissociative chemisorption processes), and that catalysis occurs at the border of these patches of surface atoms and molecular adducts (FIG. 5a). Ertl and colleagues identified the active sites for dissociative adsorption of N bonds from molecular nitrogen (and the subsequent formation of ammonia) and CO oxidation catalysis on metal surfaces[25,114,115,126]. In the CO oxidation work, for example, he and his team showed that the structure of the step sites determines whether they remain active or become deactivated by oxygen atoms[25]. These iconic images largely disproved the widely held assumption of the static surface. Equally important have been the advances of the group of Gabor Somorjai to the field of surface science. His contributions to the field of surface science and catalysis were mainly made using techniques like low-energy electron diffraction[127] and, later, on sum frequency generation[128,129]. The culmination of this low-energy electron diffraction and sum frequency generation work was the realization that surfaces are not simply restructured but clustering occurs, which strongly affects the translation between surface science principles and actual heterogeneous catalysis[130]. For example, they determined that bond activation occurs at the same time as metal sites restructure around the adsorption site, and, yet, that these strongly adsorbed molecules remain mobile[118].

As mentioned, the limits of many of the above-described surface science techniques are that they operate under strongly simplified conditions in terms of pressure, temperature, timescale and sample complexity. Surface science work itself shows that adsorbed molecules, let alone catalysis, behave differently at different pressures and temperatures[123,131]. Model systems are often required for such analyses and these can fail to capture important features of industrially relevant catalyst systems[132]. Thus, bridging the so-called pressure, temperature and materials gaps[133,134], to go towards in situ (simulating one or more catalytic reaction conditions at its place of measurement) or even operando measurements (operating at catalytic conditions and quantifying reaction products), has been a point of much focus[24,135–137]. It should be noted that, for example, the development in microelectromechanical systems is allowing more and more in situ applications of surface science techniques with short attenuation lengths in air when, for example, combined with electron microscopy[8,11,138–141].

Active site geometry, electronic structure and confinement are three basic principles with which much of the activity of heterogeneous catalysts can be understood and described. Yet, we have shown that they are only the proverbial tip of the iceberg with respect to the complexity of defining active sites. Take, for example, Somorjai's description of the involvement of carbonaceous overlayers, which led him to draw the comparison between enzyme and heterogeneous catalysis; "It is perhaps misleading to consider the metal alone as providing the catalytic surface, as one ought to scrutinize the surface properties of the catalyst in the presence of the reaction mixture. In this circumstance, the surface carbonaceous overlayer is likely to be an active participant in creating the active catalyst surface. The presence of an ordered overlayer eliminated the poisoning of dehydrogenation reactions (C_6H_{10} to C_6H_6)"[34]. The active participation of carbonaceous-containing species in the creation of the active site such as in the example of Somorjai, while not directly influencing the catalytic pathway, is another illustration of how complex it is to define the active site in heterogeneous catalysis. The same holds true for the methanol-to-hydrocarbons reaction, where the methanol reacts on a pool of hydrocarbons to form olefins, rather than at the initiating site of this pool, a Brønsted acid site[142,143]. Much of this insight in active site complexity we have only been able to study in the past two decades due to the emergence of various novel and improved analytical methods, including microscopy and spectroscopy techniques with high spatial and/or temporal

resolution[144,145]. Good examples are single-molecule fluorescence, where, for example, Roeffaers and colleagues studied Gibbsite-type stacked sheets of Li^{+}-Al^{3+} layered double hydroxide and its catalytic reaction with fluorogenic probe 5-carboxyfluorescein diacetate, which becomes emissive only upon catalytic hydrolysis in water-containing media or upon catalytic transesterification. They found that ester hydrolysis proceeds on the lateral {1010} crystal faces, while transesterification occurs on the entire outer crystal surface[146] (FIG. 5b). Another good example is the use of (tip-enhanced) atomic force microscopy-type techniques[9,147] such as that used by the groups of Gross and Toste, who studied the reduction and oxidation of N-heterocyclic carbenes on Pt nanoparticles of approximately 100 nm by synchrotron-radiation-based infrared nanospectroscopy (or nano-IR), with a spatial resolution of approximately 25 nm (FIG. 5c). They, thereby, showed that the sides of these nanoparticles, containing more stepped facets, were more active in the oxidation and reduction of chemically active groups on the N-heterocyclic carbenes than the flat tops of the Pt particles[148].

Taylor school of thought. It has become clear in the past decades that the complexity of the active site lies far beyond the equivalent adsorption sites as in the assumption of Langmuir. In fact, it is now known that active sites can cooperate or even communicate[149]. They are also dynamic, highly dependent on nanoscale intimacy, spillover effects and are subordinate to accessibility. There can be active site cooperation or interdependence, and, to measure these and other subtleties, new analytical techniques have been — and should be — developed.

The notion that the active site can only truly be understood under non-model conditions (in terms of pressure, temperature, complexity and time) drives our continued efforts in operando spectroscopy research, which goes hand in hand with Taylor's school of thought (BOX 3). To that end, vibrational spectroscopy (Raman and infrared spectroscopy), electronic spectroscopy (UV–vis and fluorescence spectroscopy) and various X-ray-based techniques (for example, X-ray absorption spectroscopy (XAS), X-ray diffraction (XRD), small-angle X-ray scattering and wide-angle X-ray scattering) can be applied under reaction conditions to study solid catalysts in action[8,150]. This requires the use of specially designed spectroscopy reaction cells. These methods can also be used in combination with microscopy techniques. Currently, along the spatial resolution development, the combination of, for example, coherent diffraction imaging with synchrotron techniques bring the spatial resolution of X-ray imaging down to (at the very best) a few nanometres. Third-generation and fourth-generation synchrotrons are being designed and, after optimization for operando conditions, this limit may be pushed down further[8]. Recently, laboratory-based XAS has also started becoming available[151,152]. Aside from spatial resolution, time resolution is also important, not only to directly study the active site but because the identification of reaction intermediates can tell us something about the site they react on. Reactive intermediates can have very short lifetimes, down to ~10^{-6} s. To gain relevant information about these reactive intermediates, nanosecond or femtosecond lasers could theoretically be used. However, these operate at a single wavelength (or narrow band), which ensures that, for full spectral information, the same catalytic reaction step should be measured multiple times at different wavelengths. Practically, this limits the application of so-called pump–probe techniques to catalytic reactions that may be reversibly onset by a pulse of some sort. This is inherently not the case for classical heterogeneous catalysts. Pump–probe techniques are ideally suited for the study of reactions that are initiated by light and, therefore, most examples can be found in the field of photocatalysis. A more broadly applicable trigger is temperature, which could technically be achieved using a short laser pulse. Yet, the effect of hot electrons on heterogeneous catalysis should be taken into account here, and, as such, this is not a straightforward method for complex (generally not fully reversible) heterogeneous catalytic reactions.

The coupling of relevant in situ or operando spectroscopies (for example, X-ray absorption, Fourier transform infrared (FTIR) and UV–Vis spectroscopy for their relative ease of use and broad applicability) with computational methods like DFT has yielded important insights in many types of catalytic systems[143,153]. An example is the much debated active site in the conversion of methane to methanol, which typically takes place in Cu-exchanged zeolite (FIG. 2). In situ vibrational and electronic spectroscopy, later in combination with DFT simulations, have granted a unique insight into the complex, enzyme-like structure of the active site in this reaction in work by Schoonheydt and colleagues[154–156]. The potential of X-rays to solve active site structures is undeniable, but great care must be taken, as the energy of the synchrotron photons necessary for many measurements may introduce artefacts in the measurements[157,158]. Validation through a combination of several techniques and, preferably, also setups or laboratories is important. The coupling of in situ aberration-corrected scanning transmission electron microscopy with XAS is an excellent example, such as that used by Hutchings and colleagues to study active sites for gold cations on a commercial hydrochlorination catalyst[51]. The team found that highly active catalysts are comprised of single-site cationic Au entities, which are analogues of single-site homogeneous Au catalysts.

Vibrational spectroscopy requires lower energy photons than X-rays and, hence, the chances of interfering with the catalyst system under study are lower. Historically, FTIR spectroscopy has been an important tool to identify actives sites of zeolite catalysis due to the excellent visibility of the active sites characterized by O–H stretching vibrations, which align well with theoretically calculated values[159]. Nevertheless, an important limitation of vibrational spectroscopy techniques is the detection limit. Particularly for Raman spectroscopy, which can, for example, be used to study carbon bonds to metal surfaces, the detection limit is relatively low. To this end, surface-enhanced techniques such as shell-isolated nanoparticle-enhanced Raman spectroscopy or tip-enhanced Raman spectroscopy

Operando spectroscopy
Operando spectroscopy studies the reaction while it takes place and is accompanied by the quantification of the reaction products, thereby allowing the direct correlation between structure and performance.

are being developed that improve the detection limit of this vibrational spectroscopy technique up to single molecules[160–163]. In recent work, Hartman et al. applied shell-isolated nanoparticle-enhanced Raman spectroscopy with isotopic labelling to distinguish surface carbonyls from formyl species on supported Rh and RhFe catalysts in the conversion of syngas to hydrocarbons[164].

Box 3 | **The operando approach and single-atom counting**

The operando approach is a methodology launched in the early 2000s that recognizes that real structure–performance correlations can only be made while the catalyst is at work[150,194,229–235]. Operando spectroscopy studies the reaction while it takes place, and is accompanied by the quantification of the reaction products, thereby, allowing the direct correlation between structure and performance. It is quite literally the attempt to bring the spectrometer to the reactor and has led to the unravelling of many complicated reaction and deactivation mechanisms. As discussed in BOX 1, the methanol-to-olefins reaction is believed to be catalysed by a Brønsted acid site. Nevertheless, in recent years, operando spectroscopy has made it clear that, in fact, the products are formed on a so-called 'hydrocarbon pool' (the dual-cycle mechanism for methanol to hydrocarbons that postulates that there are two competing cycles for ethylene and propylene formation running in the zeolite channels governed by olefins and aromatics, both acting as co-catalysts for methanol to hydrocarbons and being active hydrocarbon pool species)[143,236], which is itself created by the Brønsted acidity (see the figure, part **a**). Strictly speaking, then, the catalyst is this pool of hydrocarbon species, rather than the zeolite itself. Certainly, there is not a linear relationship between the availability and strength of Brønsted acidity and activity. The presence of too many or too strong active sites leads to catalyst deactivation by coke formation in much the same way as in fluid catalytic cracking[237] (BOX 1). It has recently been shown by operando spectroscopy (UV–vis) and X-ray diffraction that zeolite frameworks expand up to 0.9% by the formation of aromatic hydrocarbon pool molecules (like (methylated) naphthalenes and pyrene species[238] (see the figure, part **b**). Hydrocarbon species corresponding to UV–vis absorbance bands are shown, such as tetramethylnaphthalene and pyrene, in comparison with the size of the chabazite and DDR cages. These are plausible hydrocarbon pool molecules causing lattice expansion, which was observed in X-ray diffraction. Furthermore, single-atom spectroscopic experiments with similar types of zeolite systems have proven useful. Using atom probe tomography, we are now able to map, in three dimensions, the carbon in this hydrocarbon pool and other light atoms (Si, Al) that are important in the reaction, as shown in figure part **c**. The large black dots represent the ^{13}C cluster atoms and the smaller red dots represent all ^{13}C ions. By superimposing clustering of atoms, correlations can be made between atoms of deactivating species and a local increase in Brønsted acidity.

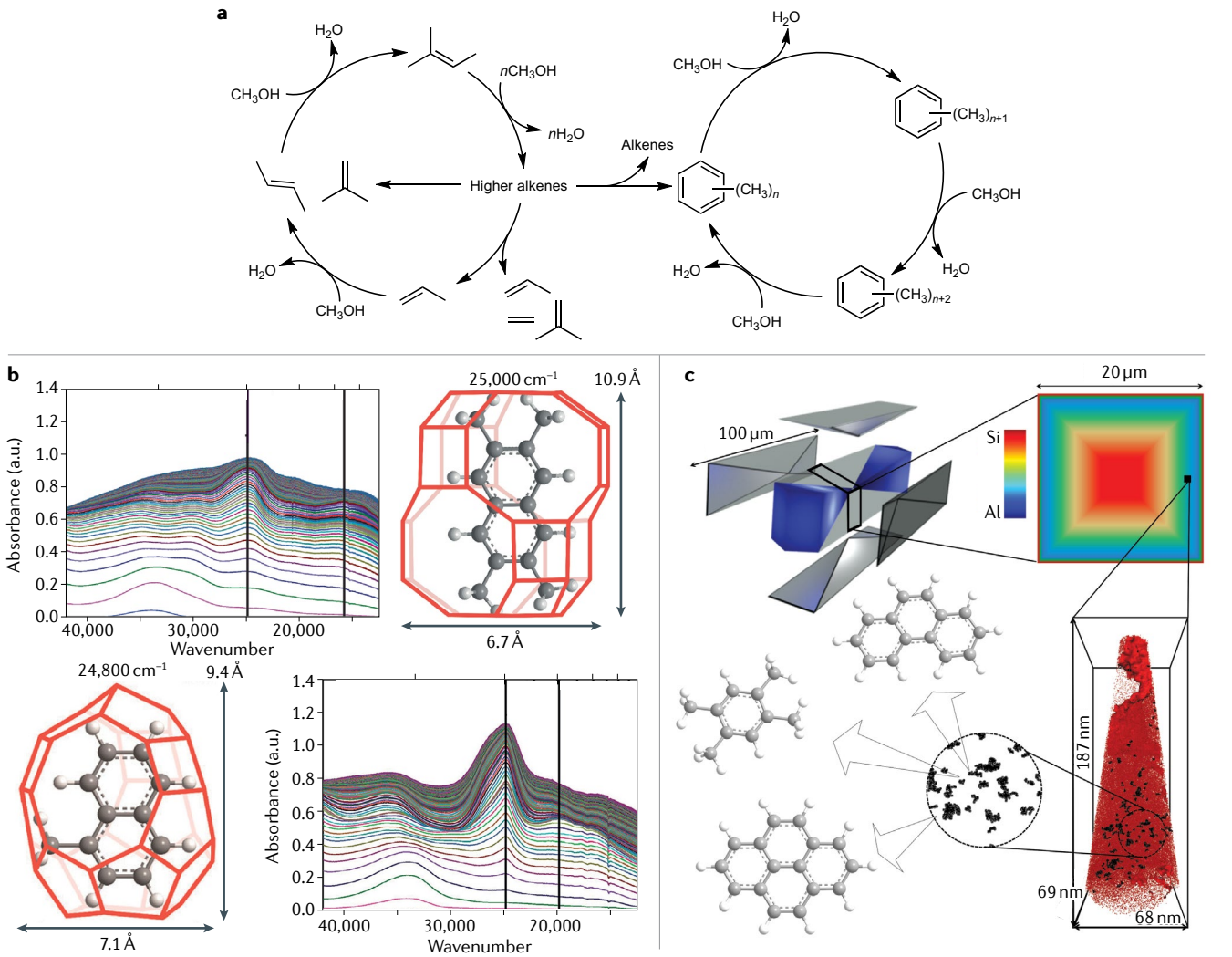

Part **a** is adapted with permission from REF.[236], Springer Nature Limited. Part **b** is reprinted with permission from REF.[238], ACS. Part **c** is adapted with permission from REF.[239], Wiley.

Chen and colleagues showed that active sites can communicate via the likely hopping of positively charged holes over a single Pd or Au nanocatalyst[149]. In this work, the fluctuations in the temporal dynamics of activity phenomena on single-particle catalysts were correlated with one another (FIG. 6a). By applying single-molecule, super-resolution mapping of fluorogenic catalytic reactions and testing their correlation in time via the computation of Pearson's cross-correlation coefficient, it was found that catalytic turnovers 'communicate' (the cross-correlation coefficients are significantly more positive than would be seen in a randomized situation) with each other over length scales of up to hundreds of nanometres. The likely underlying phenomenon, proton hopping, was directly observed by Ristanović et al., who applied fluorescence microscopy to visualize the Brønsted-acid-catalysed oligomerization of styrene derivatives in H-ZSM-5 zeolite crystals, thereby, visualizing proton transfer processes at the single-molecule level[165] (FIG. 6b). By quantifying the individual fluorescent reaction products, they were even able to estimate averaged TOF for the oligomerization reactions. Such studies with fluorogenic catalytic reactions combined with high (or super)-resolution microscopy, along with relatively homogeneous catalytic sites (such as Brønsted acidity in zeolites) are arguably the closest one can currently get to visualizing the active site at work. Chen and colleagues also showed that sites can have temporal activity fluctuations as a result of catalysis-induced and spontaneous surface restructuring[166] (FIG. 6c). Hydrogen spillover onto the support is a great example of active site cooperativity. Karim et al. showed that, on the reducible support TiO_2, hydrogen can travel tens of nanometres from a platinum nanoparticle to reduce an iron oxide particle. Here, an ingenious model system was synthesized, where pairs of platinum and iron oxide particles with varying interparticle distances were placed on a single support[167]. By applying spatially resolved XAS, the researchers were able to directly observe chemical transformations induced by hydrogen spillover. The effect of the reducibility of the support was proven by also studying a non-reducible support (Al_2O_3). Here, the hydrogen spillover distance was limited to a few nanometres, and the hydrogen diffused at much slower rates (1.4×10^{-23} cm s^{-1}, 10^{10} times slower than for TiO_2).

Another parameter that adds to the complexity of (defining) the active site, is nanoscale intimacy. For example, nanoscale intimacy in the spatial organization between two sites of a bifunctional catalyst has been shown to be extremely important, as investigated by Zecevic et al.[168]. The catalyst system that was studied is one that is important in the hydrocracking of fossil and renewable hydrocarbon sources to provide high-quality diesel fuel. It consists of an intimate mixture of zeolite Y with alumina binder and platinum metal nanoparticles, where it was long thought that the closer the platinum was to the acid sites, the better (FIG. 6d). By combining precise catalyst preparation procedures with high-resolution electron microscopy, they showed that the optimal distribution of Pt is not 'the closer the better' to the acid site on zeolite Y. Rather, for optimal hydrocracking activity and selectivity, the platinum should be located at nanoscale distance from the zeolite and on the binder[168]. This is a good example that illustrates that, with improved characterization techniques, over the last decade, the complexity of the microenvironment of active sites is only starting to be understood. The group of Ding Ma has recently shown two excellent examples of the application of such principles in interfacial catalyst design, greatly increasing the activity of two different reactions[169,170]. By combining α-MoC with atomic layered gold clusters, highly active, low-temperature, water-gas shift catalysts were obtained[169], while modifying α-MoC led to highly active hydrogen production catalysts from methanol[170].

Titrating active sites

From the above discussion, a pertinent question might be: is it possible to define and count the active sites in a catalyst? In the following, we will provide our perspective. The use of probe molecules, such as CO for metal sites or pyridine or ammonia for acid sites, in combination with spectroscopic techniques has become a well-established methodology to titrate the active site[171]. In reality, the use of any probe molecule other than the reactant itself may lead to ambiguities. Furthermore, these methods to probe the active site are, by their nature, static, whereas the active sites are in constant flux and differ locally throughout catalyst samples (BOX 3).

Let us begin, then, with a thought experiment, working under the reductionist approach that the catalytic activity of a metal nanoparticle can be found by the superimposition of the reactivity of each of the separate facets (that is, the Langmuir approach). Re-examining the data from earlier work on CO_2 reduction over a nickel catalyst[71], the weighted average of CH_4 production can be deduced from a microkinetic model. Supplementary Table 1 lists these values on different nickel facets (terraces Ni(100) and Ni(111), and stepped facet Ni(110)). In this simple simulation, it is interesting to see that the weighted average production rate increases with decreasing particle size, in accordance with experimental results[12]. FIGURE 7 shows the reaction pathways for the carbide mechanism over three different facets (Ni(111), Ni(100) and Ni(211)). The middle panels show Wulff-constructed nickel nanoparticles of different particle size diameters using the surface energies of three facets. The bottom graph shows some of the values also listed in Supplementary Table 1. This (over)simplified example (FIG. 7) directly illustrates the difficulty in assigning one active site in supported metal catalysts; if we take the 2-nm Wulff-constructed nanoparticle as an example, 80% of the total methanation activity of the particle can be attributed to stepped sites on Ni(110). It could be argued, then, that Ni(110) contains 'the (most) active methanation site'. Yet, for a 16-nm particle, while Ni(110) still has the highest CH_4 production rate, it only contributes 33% to the overall activity. In a similar thought experiment, one can think of a 'selectivity Taylor ratio', since not all active sites will preferentially produce the same product (for example, methane or CO) or produce it at the same reaction speed. It is also important to realize that these Taylor ratios are dynamic and, therefore, may change as a function of reaction time, as

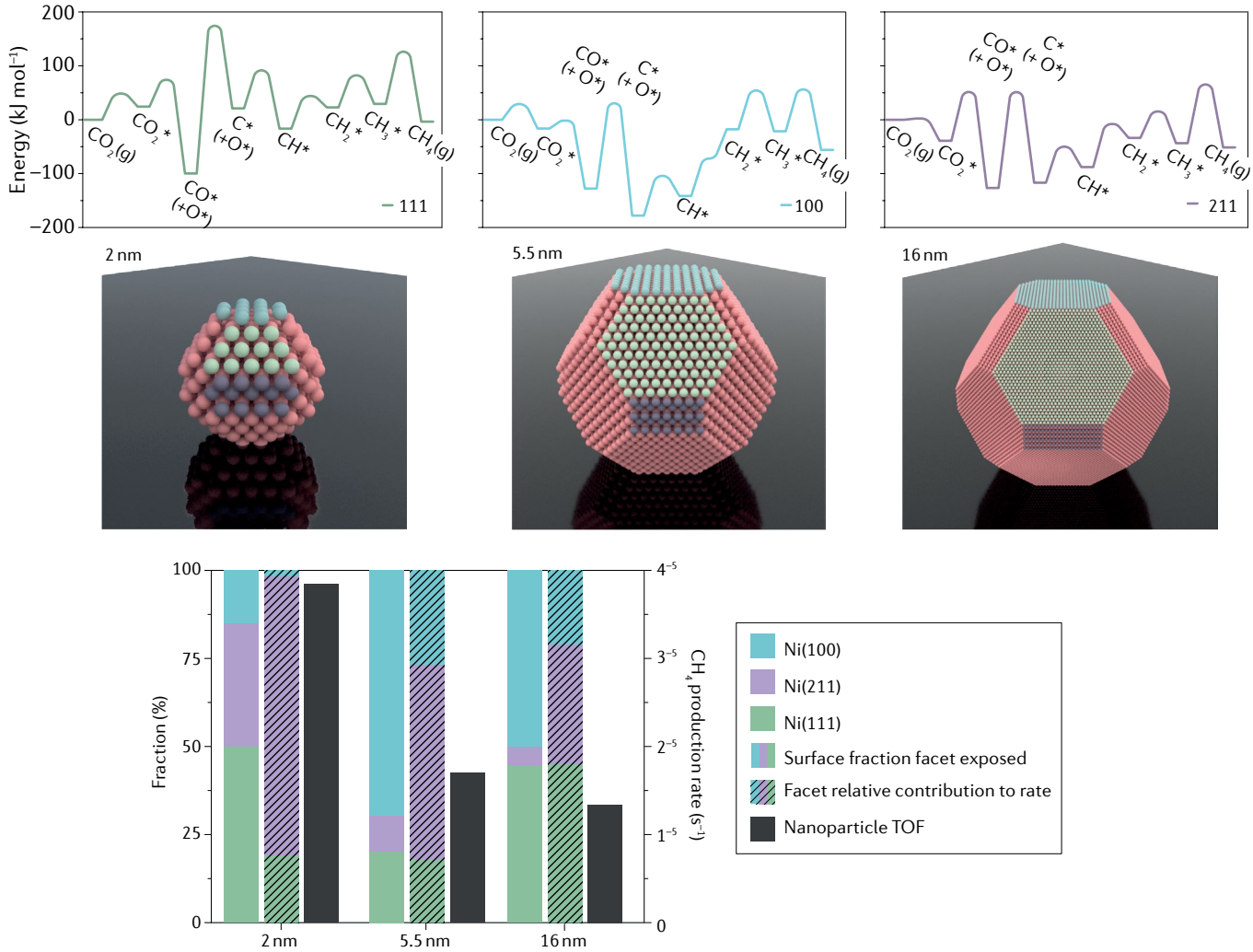

Fig. 7 | **Energy profiles of different CO_2 hydrogenation pathways over nickel.** Wulff constructions of nickel nanoparticles of different sizes (input are the surface energies of Ni(100), Ni(111) and Ni(211) at 2.21, 1.92 and 2.29 J m^{-2}, respectively). The bottom panel shows the fraction of exposed surface facets for the Wulff-constructed nanoparticles, the contribution of these facets to the overall reaction rate and the overall reaction rate. TOF, turnover frequency. Based on data from REF.[12].

shown by Vendelbo et al. with their in situ transmission electron microscopy studies[24].

Owing to a combination of known or unknown atomic or electronic defects[76], the different exposed crystallographic planes in supported metal nanoparticles[172–174], known or unknown impurities, including promoters and poisons, and reversible and irreversible phase changes induced by catalytic time on stream, the availability of different active sites on any given real catalyst ensure a plethora of (active) sites. Because of the many sites that comprise a catalyst (particularly when considering supported metal catalysts rather than on single-site catalysts or solid acids), hundreds of reaction pathways are possible, and, in many cases, hundreds of elementary reaction steps[175], from different reaction pathways, all of which are occurring at the same time. In the end, what is often termed the 'active site' is really the site with the lowest energy pathway for the rate determining step(s). Such sites will make a significant contribution to the overall rate of formation of one or more reaction products, while not necessarily being the only contribution[13]. It is important to note that this 'active site' may not be active at all if the surrounding less active sites, such as sites that are more active in preceding low-energy elementary reaction steps, aren't there. Which brings us to the main question of defining the active site, irrespective of whether the fraction of sites that are not identified as 'active sites' should be rendered as useless or inactive (as is postulated by the Taylor ratio). In reality, the picture is likely to be more subtle (FIG. 8). A metal nanoparticle has many different sites (FIG. 8a), terraces may be more active in an adsorption step, whereas edges might be more active in the rate determining bond cleavage. In a zeolite, the most active site might also be the site that is deactivated fastest by coke formation (FIG. 8b). The overall picture of the 'active site' should, therefore, rather be a weighted distribution of activity among different active sites; an average of the activities of each available site for each reaction step, weighted by the importance (relative energy barrier) of that step, and the fractional occurrence of that site.

Even if we assume the absence of heat and mass transfer, poisoning, deactivation and activation, measuring

the active site is still not straightforward. Typically, the actual 'active site' where the seemingly simple scission and formation of chemical bonds occur will be on the spatial order of a few Ångstrom (10^{-10} m), but affected by, for example, confinement on the nanometre to micrometre scale (10^{-9}–10^{-6} m), and shaped into catalyst bodies of centimetres (10^{-2} m), in reactors of metres, in chemical industry cities of multiple kilometres (10^{3} m) wide (FIG. 1). They also operate at catalytic turnovers ranging from a few ms to s (10^{-2}–10^{2} s), with reactants and products diffusing on timescales from ms to s, on surfaces and in pores, activating for hours to weeks[176,177], slowly deactivating over hours to months, and even up to 3–8 years for many industrial fixed-bed catalysts. Taking into account that chemisorption-induced restructuring can take place in less than 10^{-6} s (REF.[117]), the limits of spatially and temporally resolved operando spectroscopy and (spectro)microscopy must stretch in order to gain real-time information on the active site. Aside from the spatiotemporal challenges, a challenge exists in the distinction between spectator species versus active species. It is also most likely not an absolute distinction, owing to the complex nature of catalytic reactions and to their dynamic nature, as mentioned in detail above[33].

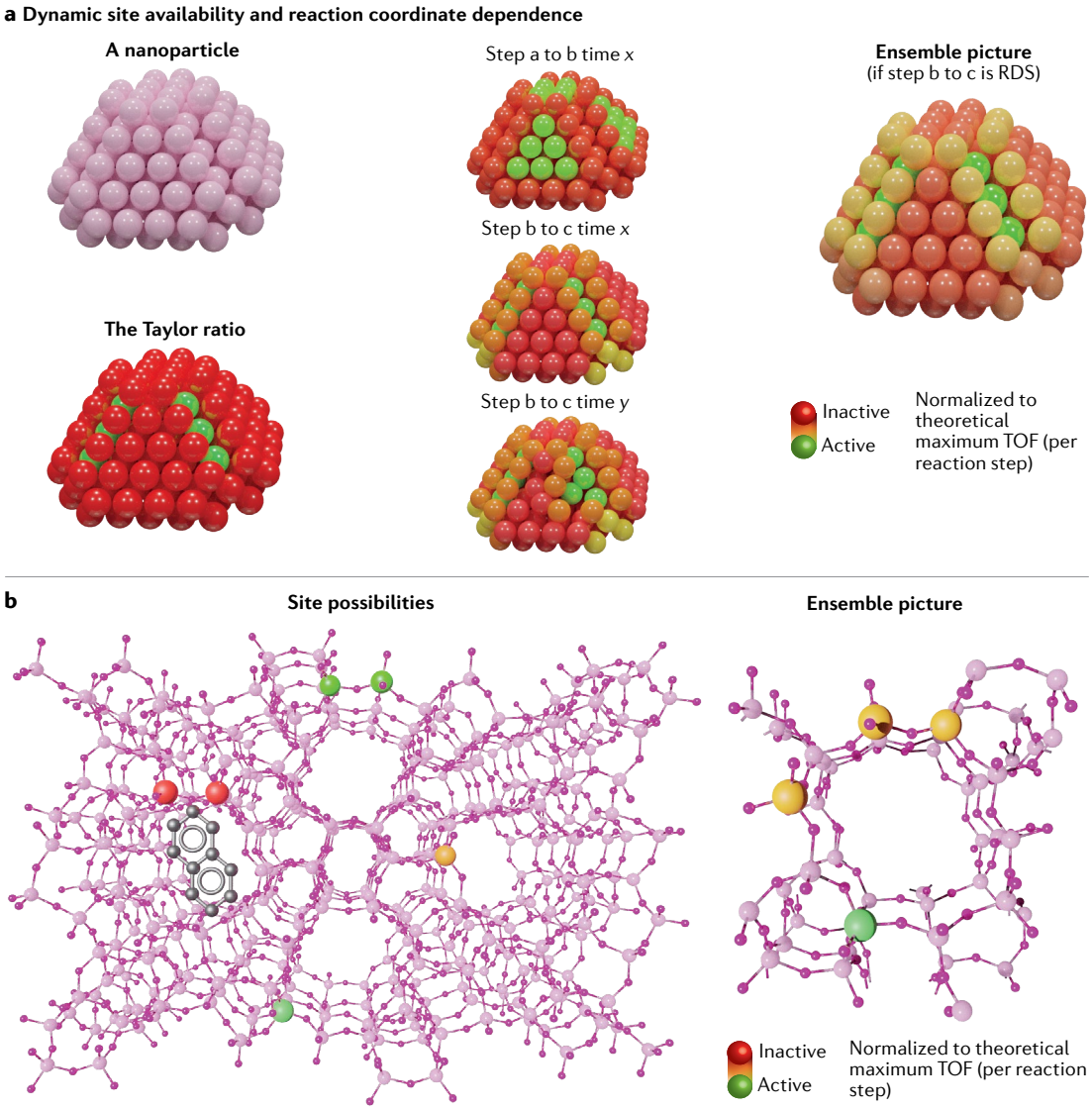

Fig. 8 | **Schematic illustrating the inherent ambiguity in assigning an active site. a** | Even if we ignore interactions with the support, a nanoparticle has many different sites that may participate in catalysis. The Taylor ratio assumes that sites are either active or non-active, whereas, in reality, the ensemble picture is far more complex and is based on dynamic site availability (including, for example, deactivation and restructuring), as well as differing activity of different sites for each fundamental reaction step. **b** | For a solid acid catalyst, each position (T site) in a zeolite ring may have different activity towards different fundamental reaction steps. In addition, different parts of a zeolite crystal may block sooner than others by the formation of, for example, polyaromatics (coke), inhibiting further reactants from penetrating into the zeolite pores to react with the solid acid sites. The ensemble picture one is left with is a distribution of activity among different sites, leaving it incorrect to assign the 'active site', as these are spatiotemporally changing in their relative amounts, accessibility and reactivity. RDS, rate determining step; TOF, turnover frequency.

But how does one experimentally measure this ensemble, dynamic picture, bearing in mind that intermediates in the most active pathway will have the shortest lifetime? It is very difficult, impossible even, to detect reaction intermediates with common characterization techniques, like gas chromatography or mass spectrometry[178], because they do not, by definition, desorb from the surface in appreciable or measurable quantities.

Operando or in situ spectroscopy, where the catalyst is studied under realistic working conditions, has proven to be important[54,179–184], and many of the recent studies that, ultimately, elucidate catalytic mechanisms, and, thereby, yield insight into the active site, combine theory with experiment for the different types of heterogeneous catalysis; Brønsted and Lewis acid catalysis, redox catalysis and (supported) metal catalysis. Yet, much work is still to be done moving towards studying systems with high complexity, such as supported metal catalysts, which, for several fundamental reasons, are particularly complex to study. First, the fraction of exposed surface on a nanoparticle is low. Of that small fraction of surface, an even smaller fraction is active. There is generally a low signal-to-noise ratio. Second, the variety of adsorption sites is large and ill-defined, and there are multiple surface elementary processes happening in tandem. There are generally broad and convoluted spectroscopic signals. Third, relevant surface processes consist of several consecutive elementary reaction steps. The adsorbate–surface systems change dynamically, which is system-inherent and, thus, desirable to study. Experimentally, this is highly challenging, particularly so considering the first and second points, as catalytic surfaces are in varying states of dynamic equilibrium.

Isotopic labelling and modulated experiments (in the form of steady-state isotopic kinetic analysis or similar experimental setups) are important experimental tools to distinguish between active and non-active or not-so-active species. A posteriori data analysis techniques, such as multivariate analysis (MVA), are also becoming increasingly important tools to distinguish between active and spectator species in complex catalytic systems. When combined with intelligent experimental design, such as the periodic and repetitive excitation of a sample of interest with an external stimulus, other data analysis techniques can be applied. An example is phase-sensitive detection, where the periodic changes within the sample can be demodulated from what does not change in the experiment[185–187]. One is, thus, in principle, able to separate bulk from surface and spectator species from active ones. It is noted here that the added value of modulated excitation experiments is no more than other a posteriori data analysis techniques such as MVA, for example, principal component analysis and clustering. Yet, in XAS, phase-sensitive detection is unique because it provides the single-atom scattering contribution already subtracted from a spectrum.

It is clear that the nature of catalytic reactions and active sites is incredibly complex, as they can even cooperate or communicate, active sites are dynamic, dependent on nanoscale intimacy, spillover effects and are subordinate to accessibility. Dynamic operando spectroscopic experiments coupled with MVA can yield new 'active site titration' methods, for example, by modulation of reactants[12,188]. Such experiments should be more widely employed now that we have available the data analysis techniques to handle the output.

For example, by applying an external stimulus in a modulating fashion to catalytic reactions in operando spectroscopy, one may theoretically be able to deduce the fraction of sites participating in the active reaction steps. In FIG. 9a–d, an example of this 'active site titration' is given for a supported metal catalyst system, in this case, CO_2 methanation (the Sabatier reaction) over Ni/SiO_2 (REF.[12]). Reactant gases were pulsed over the catalyst under reaction conditions and the catalyst ensemble was studied by quick-XAS. FIGURE 9c shows the TOF trend with particle size as reported in REF.[12]. In FIG. 9d, we have taken the peak position in FTIR for the maximal peak observed for different particle sizes and plotted it against the TOF. The resulting volcano-type plot is an excellent example of the Sabatier relationship (the bond strength of CO shows an optimum) in this Sabatier reaction. If one then takes the percentage of change in metallic nature of the different mean nickel particle sizes during the X-ray absorption experiments shown in FIG. 9a,b, we can deduce the quantity of atoms that are participating. FIGURE 9 also plots a schematic showing that, according to this deduction, the most active particle also has the most surface atoms affected by, or participating in, the experiment. It is very interesting to note that only a small fraction of the surface seems to respond to the catalytic reactants, and this observation is one along the line of Taylor's school of thought. This is one of the first examples of how, by using state-of-the-art high-time-resolution spectroscopy, one can directly probe the atoms participating in the catalytic reaction, showing that only a few of the available surface sites participate.

Concluding remarks and outlook

The key to designing new or better heterogeneous catalysts from first principles is to understand the active site not in spite of but including the full complexity and related multidimensionality of heterogeneous catalysis, that is, bridging the different dimensional scales that are of importance, including the real reaction conditions (such as temperature, pressure and time, in other words, long-term studies and high time resolution) and so forth. Here, we have explored a selection of historical as well as recent scientific contributions to the effort of understanding the concept of active site. This manuscript has focused mainly on heterogeneous thermocatalysis, which is responsible for more than 80% of catalysis currently and historically applied[189]. Nevertheless, the ongoing energy transition and subsequent electrification will likely make it that photocatalysis and electrocatalysis become increasingly important, and experimental verification must be done to ensure that the concepts discussed in this work also apply to these fields and to uncover new relevant concepts[190–193].

The Taylor ratio was defined originally as the fraction of surface atoms that are active in a catalytic reaction, compared with all the exposed surface atoms[27]. We have

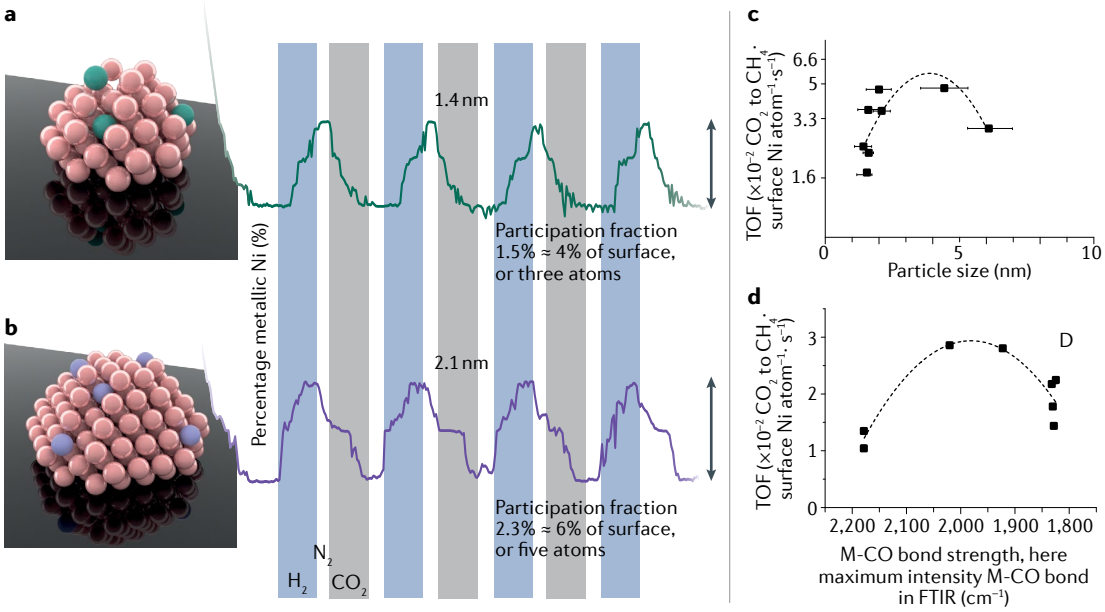

Fig. 9 | **Overview of CO_2 reduction over SiO_2-supported Ni.** In the recent literature[12], pulses of reactants in CO_2 methanation were used to determine how the electronic properties of different mean nickel particle sizes are influenced. From these data, we have determined here the surface fraction of atoms participating in the catalytic reaction shown for two particle sizes, 1.4 nm (part **a**) and 2.1 nm (part **b**). The turnover frequency (TOF) plotted against particle size (part **c**). The M-CO bond strength as determined by Fourier transform infrared (FTIR) displayed in REF.[12] plotted against the TOF (part **d**). Parts **a**, **b**, and **c** are reprinted with from REF.[12], Springer Nature Limited.

shown that this definition does not fully stretch to real systems. While the contribution of surface science to a fundamental understanding of the active site in heterogeneous catalysis has been undeniable and impressive, and is still of great importance, the often necessary simplifications in terms of time, temperature and pressure, as well as catalyst, chemical and structural complexity do not enable us to capture the full, complex reality of a catalytic process and, thus, the active site. In light of these complexities and the dynamic nature of catalytically active sites, as well as several discussed factors like their cooperation and communication between active sites, one should question if there really is such a thing as the Taylor ratio or even an active site. In light of all that is discussed, we understand that we must include much more than the classical 2D view. That is, there is at least also a volume fraction that should be taken into account. See, for example, the active site in an enzyme or, in terms of heterogeneous catalysts, the fraction of accessible zeolite cages displayed in BOX 3. It is also worth explicitly mentioning that, in applied heterogeneous catalysis, this volumetric Taylor ratio changes greatly with time.

Thus, to truly define the active site, one must take into account the multidimensional and non-absolute Taylor ratio, a weighted distribution of activity among different active sites (FIG. 8). Practically, one may wish to define the TOF not (only) per gram of catalyst but per volume and dynamic time unit, taking into account also the changes that occur during the lifetime of a catalyst. We should strive to discuss the activity of the 'active site' as an average of the activities of each available site for each reaction step, weighted by the importance (relative energy barrier) of that step and the fractional occurrence of the site. This all has to be done during the birth (activation period), life (active period) and death (deactivation period) of a catalyst. To truly measure all dimensions of the active site, a wide range (and combination) of sensitive characterization techniques is then clearly required. We should be aware that relying on generalized activity measures, such as the TOF, might very well cloud many of the details necessary to gain full understanding of active sites and the related mechanistic pathways of reactivity and deactivation. Claims of having determined the 'active site' in a catalytic reaction without respecting plausible site diversity must be relativized. They help us to define the bottom lines of our thinking, but certainly do not fully grasp the complex reality of a catalytic process.

The activity of a catalyst may typically be manipulated by 1–1.5 orders of magnitude by using geometric factors alone. By investigating different (combinations) of metals, this can be expanded to at least 2 orders of magnitude. There is obviously much to be gained in the typical 10^{-2}–10^{2} s^{-1} TOF range for man-made industrial catalysts when compared with the TOF values of 10^{3}–10^{7} s^{-1} seen for enzymes (though it is worth noting that enzymes are less active per volume)[87–90]. To achieve this, new synthesis methods and concepts should be introduced, as the scaling relations have to be breached[86]. By manipulating the electronic (for example, with multimetal sites) and geometric (for example, with ligand-like chemistries) effects, coupled with tailored confinement properties for the desired reactant, transition state and product via catalysis and process technology, we may begin to approach the activity of nature's highly evolved enzyme catalysts in the future. Yet, the realization must always be made that catalysis is part of a much larger complex whole. The translation

of this knowledge, once obtained, to catalyst synthesis or upscaling in process technology is a challenge of its own.

The full complexity of heterogeneous catalysis should be explored in a multiscale scientific approach, and subsequently designed in a way that relates to nature's fully evolved catalysts; enzymes[194,195]. Nature has optimized enzymes for millions of years, compared with which current materials science and engineering is still in its infancy[87]. Small molecule activation, such as N_2, H_2O and CO_2 activation, is one of the most pressing fields in the clean energy transition and current solid catalysts are often not active and/or not selective enough to be considered economically viable[196,197]. Taking advantage of the concepts that are developed in nature, such as active site isolation, confinement, cascading and compartmentalization, may allow overcoming some of the scientific challenges that the catalysis community currently faces, making use of established knowledge and techniques from heterogeneous catalysis, while more and more chemistry becomes electrified[191,198–203]. Selective suppression of, for example, hydrogenation activity is one of the biggest challenges in catalysis research in the activation of small molecules. In, for example, the electrocatalytic reduction of CO_2 or electrocatalytic ammonia production, the hydrogen evolution reaction competes fiercely for faradaic efficiency for all known catalyst systems[204]. In designing new catalysts for these challenges that society faces, it is important to define best practices for 'active site' determination for these side reactions. This could allow us, for example, to later on selectively position them in a catalyst reactor system. As such, it is likely that the fields of heterogeneous, enzymatic and homogeneous catalysis will continue to merge when we gain more insights into what active sites are required to perform a specific but complex chemical process.

Published online: 06 January 2022

1. Statista. *Global Chemical Industry Revenue 2019* (Statista, 2019).
2. de Jong, K. P. in *Synthesis of Solid Catalysts* (ed. de Jong, K. P.) 111–134 (Wiley, 2009).
3. Kung, H. H. & Kung, M. C. En route to complete design of heterogeneous catalysts. *Top. Catal.* **34**, 77–83 (2005).
4. Zaera, F. The new materials science of catalysis: toward controlling selectivity of the active site. *J. Phys. Chem. Lett.* **1**, 621–627 (2010).
5. Davis, M. E. Molecular design of heterogeneous catalysts. *Stud. Surf. Sci. Catal.* **130**, 49–59 (2000).
6. Hernández Mejía, C., van Deelen, T. W. & de Jong, K. P. Activity enhancement of cobalt catalysts by tuning metal-support interactions. *Nat. Commun.* **9**, 4459 (2018).
7. Zaera, F. Nanostructured materials for applications in heterogeneous catalysis. *Chem. Soc. Rev.* **42**, 2746–2762 (2013).
8. Meirer, F. & Weckhuysen, B. M. Spatial and temporal exploration of heterogeneous catalysts with synchrotron radiation. *Nat. Rev. Mater.* **3**, 324–340 (2018).
9. van Schrojenstein-Lantman, E. M., Deckert-Gaudig, T., Mank, A. J. G., Deckert, V. & Weckhuysen, B. M. Catalytic processes monitored at the nanoscale with tip-enhanced Raman spectroscopy. *Nat. Nanotechnol.* **7**, 583–586 (2012).
10. Weckhuysen, B. M. Preface: recent advances in the *in-situ* characterization of heterogeneous catalysts. *Chem. Soc. Rev.* **39**, 4557–4559 (2010).
11. van Ravenhorst, I. K. et al. Capturing the genesis of an active Fischer–Tropsch synthesis catalyst with operando X-ray nanospectroscopy. *Angew. Chem. Int. Ed.* **57**, 11957–11962 (2018).
12. Vogt, C. et al. Unravelling structure sensitivity in CO_2 hydrogenation over nickel. *Nat. Catal.* **1**, 127–134 (2018).
13. Nørskov, J. K. et al. The nature of the active site in heterogeneous metal catalysis. *Chem. Soc. Rev.* **37**, 2163–2171 (2008).
14. Cheng, T., Xiao, H. & Goddard, W. A. Nature of the active sites for CO reduction on copper nanoparticles; suggestions for optimizing performance. *J. Am. Chem. Soc.* **34**, 11642–11645 (2017).
15. Behrens, M. et al. The active site of methanol synthesis over $Cu/ZnO/Al_2O_3$. *Science* **336**, 893–898 (2012).
16. Kattel, S., Ramírez, P. J., Chen, J. G., Rodriguez, J. A. & Liu, P. Active sites for CO_2 hydrogenation to methanol on Cu/ZnO catalysts. *Science* **355**, 1296–1299 (2017).
17. Sabatier, P. & Senderens, J.-B. Hydrogénation directe des oxydes du carbone en présence de divers métaux divisés. *C. R. Acad. Sci.* **134**, 689–691 (1903).
18. Senderens, J.-B. & Sabatier, P. Nouvelles synthèses du méthane. *C. R. Acad. Sci.* **82**, 514–516 (1902).
19. Fechete, I. Paul Sabatier – The father of the chemical theory of catalysis. *C. R. Chim.* **19**, 1374–1381 (2016).
20. Müller, K., Fleige, M., Rachow, F. & Schmeißer, D. Sabatier based CO_2-methanation of flue gas emitted by conventional power plants. *Energy Procedia* **40**, 240–248 (2013).
21. Pauling, L. *The Nature of the Chemical Bond* (Cornell Univ. Press, 1939).
22. Vogt, E. T. C. & Weckhuysen, B. M. Fluid catalytic cracking: recent developments on the grand old lady of zeolite catalysis. *Chem. Soc. Rev.* **44**, 7342–7370 (2015).
23. Tao, F. et al. Reaction-driven restructuring of Rh-Pd and Pt-Pd core-shell nanoparticles. *Science* **322**, 932–934 (2008).
24. Vendelbo, S. B. et al. Visualization of oscillatory behaviour of Pt nanoparticles catalysing CO oxidation. *Nat. Mater.* **13**, 884–890 (2014).
25. Ertl, G. Oscillatory kinetics and spatio-temporal self-organization in reactions at solid surfaces. *Science* **254**, 1750–1755 (1991).
26. Armstrong, C. D. & Teixeira, A. R. Advances in dynamically controlled catalytic reaction engineering. *React. Chem. Eng.* **5**, 2185–2203 (2020).
27. Taylor, H. S. A theory of the catalytic surface. *Proc. R. Soc. Lond. A* **108**, 105–111 (1925).
28. Taylor, H. S. Fourth report of the committee on contact catalysis. *J. Phys. Chem.* **30**, 145–171 (1926).
29. Taylor, H. S. The activation energy of adsorption processes. *J. Am. Chem. Soc.* **53**, 578–597 (1931).
30. Ertl, G. et al. *Handbook of Heterogeneous Catalysis* (eds Ertl, G., Knozinger, H., Schuth, F. & Weitkamp, J.) (Wiley, 2008).
31. Dumesic, J. A., Huber, G. W. & Boudart, M. in *Handbook of Heterogeneous Catalysis* 2nd edn (eds Ertl, G., Knozinger, H., Schuth, F. & Weitkamp, J.) (Wiley, 2008).
32. Rase, H. F. *Handbook of Commercial Catalysts: Heterogeneous Catalysts* (CRC, 2000).
33. Védrine, J. C. Revisiting active sites in heterogeneous catalysis: their structure and their dynamic behaviour. *Appl. Catal. A Gen.* **474**, 40–50 (2014).
34. Somorjai, G. A. Active sites in heterogeneous catalysis. *Adv. Catal.* **26**, 1–68 (1977).
35. Somorjai, G. A., McCrea, K. R. & Zhu, J. Active sites in heterogeneous catalysis: development of molecular concepts and future challenges. *Top. Catal.* **18**, 157–166 (2002).
36. Desert, X., Carpentier, J. F. & Kirillov, E. Quantification of active sites in single-site group 4 metal olefin polymerization catalysis. *Coord. Chem. Rev.* **386**, 50–68 (2019).
37. Shamiri, A. et al. The influence of Ziegler-Natta and metallocene catalysts on polyolefin structure, properties, and processing ability. *Materials* **7**, 5069–5108 (2014).
38. Stürzel, M., Mihan, S. & Mülhaupt, R. From multisite polymerization catalysis to sustainable materials and all-polyolefin composites. *Chem. Rev.* **116**, 1398–1433 (2016).
39. Hlatky, G. G. Single-site catalysts for olefin polymerization. *Coord. Chem. Rev.* **199**, 235–329 (2000).
40. Velthoen, M. E. Z., Boereboom, J. M., Bulo, R. E. & Weckhuysen, B. M. Insights into the activation of silica-supported metallocene olefin polymerization catalysts by methylaluminoxane. *Catal. Today* **334**, 223–230 (2019).
41. Bossers, K. W. et al. Correlated X-ray ptychography and fluorescence nano-tomography on the fragmentation behavior of an individual catalyst particle during the early stages of olefin polymerization. *J. Am. Chem. Soc.* **142**, 3691–3695 (2020).
42. Bossers et al. Heterogeneity in the fragmentation of ziegler catalyst particles during ethylene polymerization quantified by X-ray nanotomography. *JACS Au* 1, 852–864 (2021).
43. Yashima, T., Sato, K., Hayasaka, T. & Hara, N. Alkylation on synthetic zeolites. III. Alkylation of toluene with methanol and formaldehyde on alkali cation exchanged zeolites. *J. Catal.* **26**, 303–312 (1972).
44. Angelici, C. et al. Ex situ and operando studies on the role of copper in Cu-promoted SiO_2–MgO catalysts for the Lebedev ethanol-to-butadiene process. *ACS Catal.* **5**, 6005–6015 (2015).
45. Sun, J. & Wang, Y. Recent advances in catalytic conversion of ethanol to chemicals. *ACS Catal.* **4**, 1078–1090 (2014).
46. Pomalaza, G., Arango Ponton, P., Capron, M. & Dumeignil, F. Ethanol-to-butadiene: the reaction and its catalysts. *Catal. Sci. Technol.* **10**, 4860–4911 (2020).
47. Makshina, E. V. et al. Review of old chemistry and new catalytic advances in the on-purpose synthesis of butadiene. *Chem. Soc. Rev.* **43**, 7917–7953 (2014).
48. Bin Samsudin, I., Zhang, H., Jaenicke, S. & Chuah, G. K. Recent advances in catalysts for the conversion of ethanol to butadiene. *Chem. Asian J.* **15**, 4199–4214 (2020).
49. Angelici, C., Weckhuysen, B. M. & Bruijnincx, P. C. A. Chemocatalytic conversion of ethanol into butadiene and other bulk chemicals. *ChemSusChem* **6**, 1595–1614 (2013).
50. Brogaard, R. Y. et al. Ethene dimerization on zeolite-hosted Ni ions: reversible mobilization of the active site. *ACS Catal.* **9**, 5645–5650 (2019).
51. Malta, G. et al. Identification of single-site gold catalysis in acetylene hydrochlorination. *Science* **355**, 1399–1403 (2017).
52. Brogaard, R. Y. & Olsbye, U. Ethene oligomerization in Ni-containing zeolites: theoretical discrimination of reaction mechanisms. *ACS Catal.* **6**, 1205–1214 (2016).
53. Hulea, V. & Fajula, F. Ni-exchanged AlMCM-41 — An efficient bifunctional catalyst for ethylene oligomerization. *J. Catal.* **225**, 213–222 (2004).
54. Moussa, S., Concepcio, P. & Arribas, A. Nature of active nickel sites and initiation mechanism for ethylene oligomerization on heterogeneous Ni-beta catalysts. *ACS Catal.* **8**, 3903–3912 (2018).
55. Wang, A. et al. Unraveling the mysterious failure of Cu/SAPO-34 selective catalytic reduction catalysts. *Nat. Commun.* **10**, 1137 (2019).
56. Borfecchia, E. et al. Cu-CHA–a model system for applied selective redox catalysis. *Chem. Soc. Rev.* **47**, 8097–8133 (2018).
57. Paolucci, C., Di Iorio, J. R., Ribeiro, F. H., Gounder, R. & Schneider, W. F. Catalysis science of NO_x selective catalytic reduction with ammonia over Cu-SSZ-13 and Cu-SAPO-34. *Adv. Catal.* **59**, 1–107 (2016).

58. Gordon, C. P. et al. Efficient epoxidation over dinuclear sites in titanium silicalite-1. *Nature* **586**, 708–713 (2020).
59. Yu, W., Porosoff, M. D. & Chen, J. G. Review of Pt-based bimetallic catalysis: from model surfaces to supported catalysts. *Chem. Rev.* **44**, 5780–5817 (2013).
60. Böller, B., Durner, K. M. & Wintterlin, J. The active sites of a working Fischer–Tropsch catalyst revealed by operando scanning tunnelling microscopy. *Nat. Catal.* **2**, 1027–1030 (2019).
61. Nelson, N. C., Nguyen, M.-T., Glezakou, V.-A., Rousseau, R. & Szanyi, J. Carboxyl intermediate formation via an in situ-generated metastable active site during water-gas shift catalysis. *Nat. Catal.* **2**, 916–924 (2019).
62. Therrien, A. J. et al. An atomic-scale view of single-site Pt catalysis for low-temperature CO oxidation. *Nat. Catal.* **1**, 192–198 (2018).
63. Liu, K., Wang, A. & Zhang, T. Recent advances in preferential oxidation of CO reaction over platinum group metal catalysts. *ACS Catal.* **2**, 1165–1178 (2012).
64. Bowker, M. Automotive catalysis studied by surface science. *Chem. Soc. Rev.* **37**, 2204–2211 (2008).
65. Van Spronsen, M. A., Frenken, J. W. M. & Groot, I. M. N. Surface science under reaction conditions: CO oxidation on Pt and Pd model catalysts. *Chem. Soc. Rev.* **46**, 4347–4374 (2017).
66. Alayon, E. M. C., Singh, J., Nachtegaal, M., Harfouche, M. & van Bokhoven, J. A. On highly active partially oxidized platinum in carbon monoxide oxidation over supported platinum catalysts. *J. Catal.* **263**, 228–238 (2009).
67. Avakyan, L. A. et al. Evolution of the atomic structure of ceria-supported platinum nanocatalysts: formation of single layer platinum oxide and Pt–O–Ce and Pt–Ce linkages. *J. Phys. Chem. C* **120**, 28057–28066 (2016).
68. Singh, J. et al. Generating highly active partially oxidized platinum during oxidation of carbon monoxide over Pt/Al_2O_3: in situ, time-resolved, and high-energy-resolution X-ray absorption spectroscopy. *Angew. Chem. Int. Ed.* **47**, 9260–9264 (2008).
69. Velthoen, M. E. Z. et al. The multifaceted role of methylaluminoxane in metallocene-based olefin polymerization catalysis. *Macromolecules* **51**, 343–355 (2018).
70. Meirer, F. et al. Life and death of a single catalytic cracking particle. *Sci. Adv.* **1**, e1400199 (2015).
71. Vogt, C. et al. Understanding carbon dioxide activation and carbon–carbon coupling over nickel. *Nat. Commun.* **10**, 5330 (2018).
72. Schmidt, J. E., Oord, R., Guo, W., Poplawsky, J. D. & Weckhuysen, B. M. Nanoscale tomography reveals the deactivation of automotive copper-exchanged zeolite catalysts. *Nat. Commun.* **8**, 1666 (2017).
73. Oord, R., Schmidt, J. E. & Weckhuysen, B. M. Methane-to-methanol conversion over zeolite Cu-SSZ-13, and its comparison with the selective catalytic reduction of NO_x with NH_3. *Catal. Sci. Technol.* **8**, 1028–1038 (2018).
74. Thomas, J. M. *Design and Application of Single-Site Heterogeneous Catalysts* (Imperial College Press, 2012).
75. Che, M. & Bennett, C. O. The influence of particle size on the catalytic properties of supported metals. *Adv. Catal.* **36**, 55–171 (1989).
76. Cratty, L. E. Jr. & Granato, A. V. Dislocations as "active sites" in heterogeneous catalysis. *J. Chem. Phys.* **26**, 96–97 (1957).
77. Sosnovsry, H. M. C. The catalytic activity of silver crystals of various orientations after bombardment with positive ions. *J. Phys. Chem. Solids* **10**, 304–310 (1959).
78. Farnsworth, H. E. & Woodcock, R. F. Radiation quenching, ion bombardment, and annealing of nickel and platinum for ethylene hydrogenation. *Ind. Eng. Chem.* **49**, 258–260 (1957).
79. Spilners, A. & Smoluchowski, R. *Reactivity of Solids* (Elsevier, 1961).
80. Louwen, J. N., Van Eijck, L., Vogt, C. & Vogt, E. T. C. Understanding the activation of ZSM-5 by phosphorus: localizing phosphate groups in the pores of phosphate-stabilized ZSM-5. *Chem. Mater.* **32**, 9390–9403 (2020).
81. Stanciakova, K. & Weckhuysen, B. M. Water-active site interactions in zeolite and their relevance in catalysis. *Trends Chem.* **3**, 456–468 (2021).
82. Derouane, E. G. The energetics of sorption by molecular sieves: surface curvature effects. *Chem. Phys. Lett.* **142**, 200–204 (1987).
83. Derouane, E. G., Andre, J.-M. & Lucas, A. A. Curvature effects in physisorption microporous solids and molecular and catalysis sieves. *J. Catal.* **110**, 58–73 (1988).
84. Ravi, M., Sushkevich, V. L. & van Bokhoven, J. A. On the location of Lewis acidic aluminum in zeolite mordenite and the role of framework-associated aluminum in mediating the switch between Brønsted and Lewis acidity. *Chem. Sci.* **12**, 4094–4103 (2021).
85. Ravi, M., Sushkevich, V. L. & van Bokhoven, J. A. Towards a better understanding of Lewis acidic aluminium in zeolites. *Nat. Mater.* **19**, 1047–1056 (2020).
86. Nørskov, J. K., Bligaard, T., Rossmeisl, J. & Christensen, C. H. Towards the computational design of solid catalysts. *Nat. Chem.* **1**, 37–46 (2009).
87. Hammer, B. & Norskov, J. K. Why gold is the noblest of all the metals. *Nature* **376**, 238–240 (1995).
88. Fields, M. et al. Scaling relations for adsorption energies on doped molybdenum phosphide surfaces. *ACS Catal.* **7**, 2528–2534 (2017).
89. Liu, X. et al. Understanding trends in electrochemical carbon dioxide reduction rates. *Nat. Commun.* **8**, 15438 (2017).
90. Latimer, A. A., Kakekhani, A., Kulkarni, A. R. & Nørskov, J. K. Direct methane to methanol: the selectivity-conversion limit and design strategies. *ACS Catal.* **8**, 6894–6907 (2018).
91. Bhattacharjee, S., Waghmare, U. V. & Lee, S. C. An improved d-band model of the catalytic activity of magnetic transition metal surfaces. *Sci. Rep.* **6**, 35916 (2016).
92. Larmier, K. et al. CO_2-to-methanol hydrogenation on zirconia-supported copper nanoparticles: reaction intermediates and the role of the metal–support interface. *Angew. Chem. Int. Ed.* **56**, 2318–2323 (2017).
93. Bus, E., Prins, R. & Bokhoven, J. A.van Origin of the cluster-size effect in the hydrogenation of cinnamaldehyde over supported Au catalysts. *Catal. Commun.* **8**, 1397–1402 (2007).
94. Derouane, E. G., Andre, J. & Lucas, A. A. A simple van der Waals model for molecule-curved surface interactions in molecular-sized microporous solids. *Chem. Phys. Lett.* **137**, 336–340 (1987).
95. Derycke, I. et al. Physisorption in confined geometry. *J. Chem. Phys.* **94**, 4620–4627 (1991).
96. Sastre, G. & Corma, A. The confinement effect in zeolites. *J. Mol. Catal. A Chem.* **305**, 3–7 (2009).
97. Vogt, E. T. C., Kresge, C. T. & Vartuli, J. C. Beyond twelve membered rings. *Stud. Surf. Sci. Catal.* **137**, 1003–1027 (2001).
98. Fraissard, J. in *Studies in Surface Science and Catalysis* Vol. 5 (eds Iwasawa, Y., Oyama, N. & X Kunieda, H.) 343–350 (Elsevier, 1980).
99. Derouane, E. G. Shape selectivity in catalysis by zeolites: the nest effect. *J. Catal.* **100**, 541–544 (1986).
100. Gounder, R. & Iglesia, E. The catalytic diversity of zeolites: confinement and solvation effects within voids of molecular dimensions. *Chem. Commun.* **49**, 3491–3509 (2013).
101. Liu, Y. et al. Enhancing the catalytic activity of hydronium ions through constrained environments. *Nat. Commun.* **8**, 14113 (2017).
102. Alizadeh, A. & McKenna, T. F. L. Particle growth during the polymerization of olefins on supported catalysts. Part 2: current experimental understanding and modeling progresses on particle fragmentation, growth, and morphology development. *Macromol. React. Eng.* **12**, 1700027 (2018).
103. Fu, Q. & Bao, X. Confined microenvironment for catalysis control. *Nat. Catal.* **2**, 834–836 (2019).
104. Cargnello, M. et al. Control of metal nanocrystal size reveals metal-support interface role for ceria catalysts. *Science* **341**, 771–773 (2013).
105. Somorjai, G. A. & McCrea, K. Roadmap for catalysis science in the 21st century: a personal view of building the future on past and present accomplishments. *Appl. Catal. A Gen.* **222**, 3–18 (2001).
106. Langmuir, I. The mechanism of the catalytic action of platinum in the reactions $2CO + O_2 = 2CO_2$ and $2H_2 + O_2 = 2H_2O$. *Trans. Faraday Soc.* **17**, 621–654 (1922).
107. Levy, R. B. The extraordinary life of Michel Boudart: a very personal perspective. *J. Catal.* https://doi.org/10.1016/j.jcat.2021.01.008 (2021).
108. Ertl, G. Catalysis is a kinetic phenomenon: the legacy of Michel Boudart. *J. Catal.* https://doi.org/10.1016/j.jcat.2021.01.009 (2021).
109. Boudart, M. Catalysis by supported metals. *Adv. Catal.* **20**, 153–166 (1969).
110. Boudart, M. Heterogeneous catalysis by metals. *J. Mol. Catal.* **30**, 27–38 (1985).
111. Eischens, R. P. & Pliskin, W. A. The infrared spectra of adsorbed molecules. *Adv. Catal.* **10**, 1–56 (1958).
112. Mapes, J. E. & Eischens, R. P. The infrared spectra of ammonia chemisorbed on cracking catalysts. *J. Phys. Chem.* **279**, 1950–1953 (1954).
113. Eischens, R. P. Infrared spectra of chemisorbed molecules. *J. Chem. Educ.* **35**, 385–391 (1958).
114. Wolff, J., Papathanasiou, A. G., Kevrekidis, I. G., Rotermund, H. H. & Ertl, G. Spatiotemporal addressing of surface activity. *Science* **294**, 134–137 (2001).
115. Ertl, G. Reactions at surfaces: from atoms to complexity. *Angew. Chem. Int. Ed.* **47**, 3524–3535 (2008).
116. Kleinle, G., Penka, V., Behm, R. J., Ertl, G. & Moritz, W. Structure determination of an adsorbate-induced multilayer reconstruction: (1×2)-H/Ni(110). *Phys. Rev. Lett.* **58**, 148 (1987).
117. Somorjai, G. A. The experimental evidence of the role of surface restructuring during catalytic reactions. *Catal. Lett.* **12**, 17–34 (1992).
118. Somorjai, G. A., Contreras, A. M., Montano, M. & Rioux, R. M. Clusters, surfaces, and catalysis. *Proc. Natl Acad. Sci. USA* **103**, 10577–10583 (2006).
119. Goodman, D. W. Model studies in catalysis using surface science probes. *Chem. Rev.* **95**, 523–536 (1995).
120. Vang, R. T., Lauritsen, J. V., Lægsgaard, E. & Besenbacher, F. Scanning tunneling microscopy as a tool to study catalytically relevant model systems. *Chem. Soc. Rev.* **37**, 2191–2203 (2008).
121. Liu, X., Madix, R. J. & Friend, C. M. Unraveling molecular transformations on surfaces: a critical comparison of oxidation reactions on coinage metals. *Chem. Soc. Rev.* **37**, 2243–2261 (2008).
122. Qian, J., An, Q., Fortunelli, A., Nielsen, R. J. & Goddard, W. A. Reaction mechanism and kinetics for ammonia synthesis on the Fe(111) surface. *J. Am. Chem. Soc.* **140**, 6288–6297 (2018).
123. Eren, B. et al. Activation of Cu(111) surface by decomposition into nanoclusters driven by CO adsorption. *Science* **351**, 475–478 (2016).
124. Tao, F. et al. Break-up of stepped platinum catalyst surfaces by high CO coverage. *Science* **327**, 850–853 (2010).
125. Heine, C., Lechner, B. A. J., Bluhm, H. & Salmeron, M. Recycling of CO_2: probing the chemical state of the Ni(111) surface during the methanation reaction with ambient-pressure X-ray photoelectron spectroscopy. *J. Am. Chem. Soc.* **138**, 13246–13252 (2016).
126. Zambelli, T., Wintterlin, J., Trost, J. & Ertl, G. Identification of the "active sites" of a surface-catalyzed reaction. *Science* **273**, 1688–1690 (1996).
127. Lang, B., Joyner, R. W. & Somorjai, G. A. Low energy electron diffraction studies of high index crystal surfaces of platinum. *Surf. Sci.* **30**, 440–453 (1972).
128. Somorjai, G. A. New model catalysts (platinum nanoparticles) and new techniques (SFG and STM) for studies of reaction intermediates and surface restructuring at high pressures during catalytic reactions. *Appl. Surf. Sci.* **121–122**, 1–19 (1997).
129. Somorjai, G. A. Molecular concepts of heterogeneous catalysis. *J. Mol. Struct.* **424**, 101–117 (1998).
130. Somorjai, G. A. The flexible surface: new techniques for molecular level studies of time dependent changes in metal surface structure and adsorbate structure during catalytic reactions. *J. Mol. Catal. A Chem.* **107**, 39–53 (1996).
131. Eren, B., Weatherup, R. S., Liakakos, N., Somorjai, G. A. & Salmeron, M. Dissociative carbon dioxide adsorption and morphological changes on Cu(100) and Cu(111) at ambient pressures. *J. Am. Chem. Soc.* **138**, 8207–8211 (2016).
132. Greeley, J. P. Active site of an industrial catalyst. *Science* **336**, 810–812 (2012).
133. Somorjai, G. A. & Park, J. Y. Molecular surface chemistry by metal single crystals and nanoparticles from vacuum to high pressure. *Chem. Soc. Rev.* **37**, 2155–2162 (2008).
134. Salmeron, M. & Eren, B. High-pressure scanning tunneling microscopy. *Chem. Rev.* **121**, 962–1006 (2020).
135. Oosterbeek, H. Bridging the pressure and material gap in heterogeneous catalysis: cobalt Fischer–Tropsch catalysts from surface science to industrial application. *Phys. Chem. Chem. Phys.* **9**, 3570–3576 (2007).
136. Woodruff, D. P. Bridging the pressure gap: Can we get local quantitative structural information at 'near-ambient' pressures? *Surf. Sci.* **652**, 4–6 (2016).
137. Bordiga, S., Groppo, E., Agostini, G., Van Bokhoven, J. A. & Lamberti, C. Reactivity of

surface species in heterogeneous catalysts probed by in situ X-ray absorption techniques. *Chem. Rev.* **113**, 1736–1850 (2013).
138. Li, Y. et al. Dynamic structure of active sites in ceria-supported Pt catalysts for the water gas shift reaction. *Nat. Commun.* **12**, 914 (2021).
139. Barroo, C., Wang, Z. J., Schlögl, R. & Willinger, M. G. Imaging the dynamics of catalysed surface reactions by in situ scanning electron microscopy. *Nat. Catal.* **3**, 30–39 (2020).
140. Ek, M., Ramasse, Q. M., Arnarson, L., Georg Moses, P. & Helveg, S. Visualizing atomic-scale redox dynamics in vanadium oxide-based catalysts. *Nat. Commun.* **8**, 305 (2017).
141. Ek, M. et al. Probing surface-sensitive redox properties of VO_x/TiO_2 catalyst nanoparticles. *Nanoscale* **13**, 7266–7272 (2021).
142. Goetze, J. et al. Insights into the activity and deactivation of the methanol-to-olefins process over different small-pore zeolites as studied with operando UV–Vis spectroscopy. *ACS Catal.* **7**, 4033–4046 (2017).
143. Yarulina, I. et al. Structure–performance descriptors and the role of Lewis acidity in the methanol-to-propylene process. *Nat. Chem.* **10**, 804–812 (2018).
144. Olsbye, U. et al. The formation and degradation of active species during methanol conversion over protonated zeotype catalysts. *Chem. Soc. Rev.* **44**, 7155–7176 (2015).
145. Olsbye, U. et al. Conversion of methanol to hydrocarbons: how zeolite cavity and pore size controls product selectivity. *Angew. Chem. Int. Ed.* **51**, 5810–5831 (2012).
146. Roeffaers, M. B. J. et al. Spatially resolved observation of crystal-face-dependent catalysis by single turnover counting. *Nature* **439**, 572–575 (2006).
147. Delen, G., Monai, M., Meirer, F. & Weckhuysen, B. M. *In situ* nanoscale infrared spectroscopy of water adsorption on nanoislands of surface-anchored metal-organic frameworks. *Angew. Chem. Int. Ed.* **60**, 1620–1624 (2021).
148. Wu, C. Y. et al. High-spatial-resolution mapping of catalytic reactions on single particles. *Nature* **541**, 511–515 (2017).
149. Zou, N. et al. Cooperative communication within and between single nanocatalysts. *Nat. Chem.* **10**, 607–614 (2018).
150. Weckhuysen, B. M. Operando spectroscopy: fundamental and technical aspects of spectroscopy of catalysts under working conditions. *Phys. Chem. Chem. Phys.* **5**, 1–9 (2003).
151. Moya-Cancino, J. G., Honkanen, A., Eerden, A. M. J. V. D. & Schaink, H. In-situ X-ray absorption near edge structure spectroscopy of a solid catalyst using a laboratory-based set-up. *ChemCatChem* **11**, 1039–1044 (2019).
152. Zimmermann, P. et al. Modern X-ray spectroscopy: XAS and XES in the laboratory. *Coord. Chem. Rev.* **423**, 213466 (2020).
153. Azaiza-Dabbah, D. et al. Functional models of carbon monoxide dehydrogenase enzymes: molecular transition metal oxide electrocatalysts for the reversible carbon dioxide–carbon monoxide transformation. *Angew. Chem. Int. Ed.* https://doi.org/10.1002/anie.202112915 (2021).
154. Groothaert, M. H., Smeets, P. J., Sels, B. F., Jacobs, P. A. & Schoonheydt, R. A. Selective oxidation of methane by the bis(μ-oxo)dicopper core stabilized on ZSM-5 and mordenite zeolites. *J. Am. Chem. Soc.* **127**, 1394–1395 (2005).
155. Woertink, J. S. et al. A $[Cu_2O]^{2+}$ core in Cu-ZSM-5, the active site in the oxidation of methane to methanol. *Proc. Natl Acad. Sci. USA* **106**, 18908–18913 (2009).
156. Snyder, B. E. R. et al. The active site of low-temperature methane hydroxylation in iron-containing zeolites. *Nature* **536**, 317–321 (2016).
157. Castillo, R. G. et al. High-energy-resolution fluorescence-detected X-ray absorption of the Q intermediate of soluble methane monooxygenase. *J. Am. Chem. Soc.* **139**, 18024–18033 (2017).
158. Cutsail, G. E. et al. High-resolution extended X-ray absorption fine structure analysis provides evidence for a Longer Fe · · · Fe distance in the Q intermediate of methane monooxygenase. *J. Am. Chem. Soc.* **140**, 16807–16820 (2018).
159. Catlow, A. et al. Bridging hydrodyl groups in zeolitic catalysts: a computer simulation of their structure, vibrational properties and acidity in protonated faujasites (H–Y zeolites). *Chem. Phys. Lett.* **188**, 320–325 (1992).
160. Hartman, T. & Weckhuysen, B. M. Thermally stable TiO_2 and SiO_2 shell-isolated Au nanoparticles for in situ plasmon-enhanced Raman spectroscopy of hydrogenation catalysts. *Chem. Eur. J.* **24**, 3733–3741 (2018).
161. Hartman, T., Wondergem, C. S., Kumar, N., Berg, A. V. D. & Weckhuysen, B. M. Surface- and tip-enhanced Raman spectroscopy in catalysis. *J. Phys. Chem. Lett.* **7**, 1570–1584 (2016).
162. Li, J. F. et al. Shell-isolated nanoparticle-enhanced Raman spectroscopy. *Nature* **464**, 392–395 (2010).
163. Hartman, T., Geitenbeek, R. G., Wondergem, C. S., Van Der Stam, W. & Weckhuysen, B. M. Operando nanoscale sensors in catalysis: all eyes on catalyst particles. *ACS Nano* **14**, 3725–3735 (2020).
164. Hartman, T., Geitenbeek, R. G., Whiting, G. T. & Weckhuysen, B. M. Operando monitoring of temperature and active species at the single catalyst particle level. *Nat. Catal.* **2**, 986–996 (2019).
165. Ristanović, Z., Kubarev, A. V., Hofkens, J., Roeffaers, M. B. J. & Weckhuysen, B. M. Single molecule nanospectroscopy visualizes proton-transfer processes within a zeolite crystal. *J. Am. Chem. Soc.* **138**, 13586–13596 (2016).
166. Xu, W., Kong, J. S., Yeh, Y. T. E. & Chen, P. Single-molecule nanocatalysis reveals heterogeneous reaction pathways and catalytic dynamics. *Nat. Mater.* **7**, 992–996 (2008).
167. Karim, W. et al. Catalyst support effects on hydrogen spillover. *Nature* **541**, 68–71 (2017).
168. Zecevic, J., Vanbutsele, G., De Jong, K. P. & Martens, J. A. Nanoscale intimacy in bifunctional catalysts for selective conversion of hydrocarbons. *Nature* **528**, 245–254 (2015).
169. Yao, S. et al. Atomic-layered Au clusters on α-MoC as catalysts for the low-temperature water-gas shift reaction. *Science* **357**, 389–393 (2017).
170. Lin, L. et al. Low-temperature hydrogen production from water and methanol using Pt/α-MoC catalysts. *Nature* **544**, 80–83 (2017).
171. Kobozev, N. I. A theory of the formation of catalytically active "ensembles" on surfaces. I. *Acta Physicochim USSR* **9**, 805 (1938).
172. van Hardeveld, R. & van Montfoort, A. The influence of crystallite size on the adsorption of molecular nitrogen on nickel, palladium and platinum. *Surf. Sci.* **4**, 396–430 (1966).
173. Fischer, N., Van Steen, E. & Claeys, M. Structure sensitivity of the Fischer–Tropsch activity and selectivity on alumina supported cobalt catalysts. *J. Catal.* **299**, 67–80 (2013).
174. Zhu, W. et al. Active and selective conversion of CO_2 to CO on ultrathin Au nanowires. *J. Am. Chem. Soc.* **136**, 16132–16135 (2014).
175. Ulissi, Z. W., Medford, A. J., Bligaard, T. & Nørskov, J. K. To address surface reaction network complexity using scaling relations machine learning and DFT calculations. *Nat. Commun.* **8**, 14621 (2017).
176. Vogt, C., Weckhuysen, B. M. & Ruiz-Martínez, J. Effect of feedstock and catalyst impurities on the methanol-to-olefin reaction over H-SAPO-34. *ChemCatChem* **9**, 183–194 (2017).
177. Ravenhorst, I. K. V. et al. On the cobalt carbide formation in a Co/TiO_2 Fischer–Tropsch synthesis catalyst as studied by high-pressure, long-term *operando* X-ray absorption and diffraction. *ACS Catal.* **11**, 2956–2967 (2021).
178. Zaera, F. The surface chemistry of heterogeneous catalysis: mechanisms, selectivity, and active sites. *Chem. Rec.* **5**, 133–144 (2005).
179. Yardimci, D., Serna, P. & Gates, B. C. Surface-mediated synthesis of dimeric rhodium catalysts on MgO: tracking changes in the nuclearity and ligand environment of the catalytically active sites by X-ray absorption and infrared spectroscopies. *Chem. Eur. J.* **19**, 1235–1245 (2013).
180. Kale, M. J. & Christopher, P. Utilizing quantitative in-situ FTIR spectroscopy to identify well-coordinated Pt atoms as the active site for CO oxidation on Al_2O_3-supported Pt catalysts. *ACS Catal.* **6**, 5599–5609 (2016).
181. Avanesian, T. et al. Quantitative and atomic-scale view of CO-induced Pt nanoparticle surface reconstruction at saturation coverage via DFT calculations coupled with in situ TEM and IR. *J. Am. Chem. Soc.* **139**, 4551–4558 (2017).
182. Matsubu, J. C., Yang, V. N. & Christopher, P. Isolated metal active site concentration and stability control catalytic CO_2 reduction selectivity. *J. Am. Chem. Soc.* **137**, 3076–3084 (2015).
183. Ding, K. et al. Identification of active sites in CO oxidation and water-gas shift over supported Pt catalysts. *Science* **350**, 189–192 (2015).
184. Agnelli, M., Swaan, H. M., Marquez-Alvarez, C., Martin, G. A., & Mirodatos, C. CO hydrogenation on a nickel catalyst: II. A mechanistic study by transient kinetics and infrared spectroscopy. *J. Catal.* **175**, 117–128 (1998).
185. Baurecht, D. & Fringeli, U. P. Quantitative modulated excitation Fourier transform infrared spectroscopy. *Rev. Sci. Instrum.* **72**, 3782–3792 (2001).
186. König, C. F. J., Van Bokhoven, J. A., Schildhauer, T. J. & Nachtegaal, M. Quantitative analysis of modulated excitation X-ray absorption spectra: enhanced precision of EXAFS fitting. *J. Phys. Chem. C* **116**, 19857–19866 (2012).
187. Chiarello, G. L., Nachtegaal, M., Marchionni, V., Quaroni, L. & Ferri, D. Adding diffuse reflectance infrared Fourier transform spectroscopy capability to extended x-ray-absorption fine structure. *Rev. Sci. Instrum.* **85**, 074102 (2016).
188. Maeda, N., Meemken, F., Hungerbühler, K. & Baiker, A. Spectroscopic detection of active species on catalytic surfaces: steady-state versus transient method. *Chimia* **66**, 664–667 (2012).
189. Jin, R., Li, G., Sharma, S., Li, Y. & Du, X. Toward active-site tailoring in heterogeneous catalysis by atomically precise metal nanoclusters with crystallographic structures. *Chem. Rev.* **121**, 567–648 (2020).
190. An, H. et al. Sub-second time-resolved surface enhanced Raman spectroscopy reveals dynamic CO intermediates during electrochemical CO_2 reduction on copper. *Angew. Chem. Int. Ed.* **60**, 16576–16584 (2021).
191. Timoshenko, J. & Roldan Cuenya, B. *In situ*/*operando* electrocatalyst characterization by X-ray absorption spectroscopy. *Chem. Rev.* **121**, 882–961 (2020).
192. Simon, G. H., Kley, C. S. & Roldan Cuenya, B. Potential-dependent morphology of copper catalysts during CO_2 electroreduction revealed by in situ atomic force microscopy. *Angew. Chem. Int. Ed.* **60**, 2561–2568 (2021).
193. Pei, G. X. et al. Identification of photoexcited electron relaxation in a cobalt phosphide modified carbon nitride photocatalyst. *ChemPhotoChem* **5**, 330–334 (2021).
194. Weckhuysen, B. M. Communicating catalysts. *Nat. Chem.* **10**, 580–582 (2018).
195. Ye, R., Hurlburt, T. J., Sabyrov, K., Alayoglu, S. & Somorjai, G. A. Molecular catalysis science: perspective on unifying the fields of catalysis. *Proc. Natl Acad. Sci. USA* **113**, 5159–5166 (2016).
196. Vogt, C., Monai, M., Kramer, G. J. & Weckhuysen, B. M. The renaisance of the Sabatier reaction and its applications on Earth and in space. *Nat. Catal.* **2**, 188–197 (2019).
197. She, Z. W. et al. Combining theory and experiment in electrocatalysis: insights into materials design. *Science* **355**, eaad4998 (2017).
198. Liu, L. & Corma, A. Structural transformations of solid electrocatalysts and photocatalysts. *Nat. Rev. Chem.* **5**, 256–276 (2021).
199. Stangl, A., Muñoz-Rojas, D. & Burriel, M. In situ and operando characterisation techniques for solid oxide electrochemical cells: recent advances. *J. Phys. Energy* **3**, 012001 (2021).
200. Jin, L. & Seifitokaldani, A. In situ spectroscopic methods for electrocatalytic CO_2 reduction. *Catalysts* **10**, 481 (2020).
201. Jaegers, N. R., Mueller, K. T., Wang, Y. & Hu, J. Z. Variable temperature and pressure operando MAS NMR for catalysis science and related materials. *Acc. Chem. Res.* **53**, 611–619 (2020).
202. Varsha, M. V. & Nageswaran, G. Operando X-ray spectroscopic techniques: a focus on hydrogen and oxygen evolution reactions. *Front. Chem.* **8**, 23 (2020).
203. Fabbri, E., Abbott, D. F., Nachtegaal, M. & Schmidt, T. J. Operando X-ray absorption spectroscopy: a powerful tool toward water splitting catalyst development. *Curr. Opin. Electrochem.* **5**, 20–26 (2017).
204. Hori, Y. *Electrochemical CO_2 Reduction on Metal Electrodes* (Springer, 2008).
205. Vis, C. M., Smulders, L. C. J. & Bruijnincx, P. C. A. Tandem catalysis with antagonistic catalysts compartmentalized in the dispersed and continuous phases of a pickering emulsion. *ChemSusChem* **12**, 2176–2180 (2019).
206. Isaacs, M. A. et al. A spatially orthogonal hierarchically porous acid–base catalyst for cascade and antagonistic reactions. *Nat. Catal.* **3**, 921–931 (2020).
207. Kikuchi, E., Nakano, H., Shimomura, K. & Morita, Y. Catalytic cracking of hydrocarbons with zeolite catalyst. *Sekiyu Gakkaishi* **28**, 210–213 (1985).
208. Haneda, M., Watanabe, T., Kamiuchi, N. & Ozawa, M. Effect of platinum dispersion on the catalytic activity of Pt/Al_2O_3 for the oxidation of carbon monoxide and propene. *Appl. Catal. B Environ.* **142**, 8–14 (2013).

209. Ristanović, Z. et al. Reversible and site-dependent proton-transfer in zeolites uncovered at the single-molecule level. *J. Am. Chem. Soc.* **140**, 14195–14205 (2018).
210. Ristanović, Z. et al. High-resolution single-molecule fluorescence imaging of zeolite aggregates within real-life fluid catalytic cracking particles. *Angew. Chem. Int. Ed.* **54**, 1836–1840 (2015).
211. Vesely, A. M. et al. 3-D X-ray nanotomography reveals different carbon deposition mechanisms in a single catalyst particle. *ChemCatChem* **13**, 2494–2507 (2021).
212. Bennett, C. O. & Che, M. Some geometric aspects of structure sensitivity. *J. Catal.* **120**, 293–302 (1989).
213. van Santen, R. A. Complementary structure sensitive and insensitive catalytic relationships. *Acc. Chem. Res.* **42**, 57–66 (2009).
214. Wei, J. & Iglesia, E. Structural requirements and reaction pathways in methane activation and chemical conversion catalyzed by rhodium. *J. Catal.* **225**, 116–127 (2004).
215. Mark, M. & Maier, W. F. CO_2 reforming of ethanol on supported Rh catalysts. *J. Catal.* **2**, 4–5 (1996).
216. Efstathiou, A. M., Kladi, A., Tsipouriari, V. A. & Verykios, X. E. Reforming of methane with carbon dioxide to synthesis gas over supported rhodium catalysts. *J. Catal.* **158**, 64–75 (1996).
217. Wei, J. & Iglesia, E. Mechanism and site requirements for activation and chemical conversion of methane on supported Pt clusters and turnover rate comparisons among noble metals. *J. Phys. Chem. B* **108**, 4094–4103 (2004).
218. Yu, J. et al. Facile synthesis of highly active Rh/Al_2O_3 steam reforming catalysts with preformed support by flame spray pyrolysis. *Appl. Catal. B Environ.* **198**, 171–179 (2016).
219. Ramallo-López, J. M. et al. Complementary methods for cluster size distribution measurements: supported platinum nanoclusters in methane reforming catalysts. *J. Mol. Catal. A Chem.* **228**, 299–307 (2005).
220. Feio, L. S. F. et al. The effect of ceria content on the properties of $Pd/CeO_2/Al_2O_3$ catalysts for steam reforming of methane. *Appl. Catal. A Gen.* **316**, 107–116 (2007).
221. Wei, J. & Iglesia, E. Isotopic and kinetic assessment of the mechanism of reactions of C_4 with CO_2 or H_2O to form synthesis gas and carbon on nickel catalysts. *J. Catal.* **224**, 370–383 (2004).
222. Bezemer, G. L. et al. Cobalt particle size effects in the Fischer–Tropsch reaction studied with carbon nanofiber supported catalysts. *J. Am. Chem. Soc.* **128**, 3956–3964 (2006).
223. Erdöhelyi, A., Pásztor, M. & Solymosi, F. Catalytic hydrogenation of CO_2 over supported palladium. *J. Catal.* **98**, 166–177 (1986).
224. Karelovic, A. & Ruiz, P. Mechanistic study of low temperature CO_2 methanation over Rh/TiO_2 catalysts. *J. Catal.* **301**, 141–153 (2013).
225. Schlatter, J. C. & Boudart, M. Hydrogenation of ethylene on supported platinum. *J. Catal.* **24**, 482–492 (1972).
226. Shaikhutdinov, S. H. et al. Structure–reactivity relationships on supported metal model catalysts: adsorption and reaction of ethene and hydrogen on $Pd/Al_2O_3/NiAl(110)$. *J. Catal.* **200**, 330–339 (2001).
227. Freund, H.-J. & Messmer, R. P. On the bonding and reactivity of CO_2 on metal surfaces. *Surf. Sci.* **172**, 1–30 (1986).
228. Rupprechter, G. Surface vibrational spectroscopy on noble metal catalysts from ultrahigh vacuum to atmospheric pressure. *Ann. Rep. Prog. Chem.* **100**, 237–311 (2004).
229. Bañares, M. A., Guerrero-Pérez, M. O., Fierro, J. L. G. & Cortez, G. G. Raman spectroscopy during catalytic operations with on-line activity measurement (operando spectroscopy): a method for understanding the active centres of cations supported on porous materials. *J. Mater. Chem.* **12**, 3337–3342 (2002).
230. Weckhuysen, B. M. Chemical imaging of spatial heterogeneities in catalytic solids at different length and time scales. *Angew. Chem. Int. Ed.* **48**, 4910–4943 (2009).
231. Buurmans, I. L. C. & Weckhuysen, B. M. Heterogeneities of individual catalyst particles in space and time as monitored by spectroscopy. *Nat. Chem.* **4**, 873–886 (2012).
232. Bañares, M. A. Operando spectroscopy: the knowledge bridge to assessing structure–performance relationships in catalyst nanoparticles. *Adv. Mater.* **23**, 5293–5301 (2011).
233. Bañares, M. A. *Operando* methodology: combination of in situ spectroscopy and simultaneous activity measurements under catalytic reaction conditions. *Catal. Today* **100**, 71–77 (2005).
234. Weckhuysen, B. M. Determining the active site in a catalytic process: *operando* spectroscopy is more than a buzzword. *Phys. Chem. Chem. Phys.* **5**, 4351–4360 (2003).
235. Weckhuysen, B. M. Studying birth, life and death of catalytic solids with operando spectroscopy. *Natl Sci. Rev.* **2**, 147–149 (2015).
236. Yarulina, I., Chowdhury, A. D., Meirer, F., Weckhuysen, B. M. & Gascon, J. Recent trends and fundamental insights in the methanol-to-hydrocarbons process. *Nat. Catal.* **1**, 398–411 (2018).
237. Mores, D., Kornatowski, J., Olsbye, U. & Weckhuysen, B. M. Coke formation during the methanol-to-olefin conversion: in situ microspectroscopy on individual H-ZSM-5 crystals with different Brønsted acidity. *Chem. Eur. J.* **17**, 2874–2884 (2011).
238. Goetze, J., Yarulina, I., Gascon, J., Kapteijn, F. & Weckhuysen, B. M. Revealing lattice expansion of small-pore zeolite catalysts during the methanol-to-olefins process using combined operando X-ray diffraction and UV–vis spectroscopy. *ACS Catal.* **8**, 2060–2070 (2018).
239. Schmidt, J. E. et al. Coke formation in a zeolite crystal during the methanol-to-hydrocarbons reaction as studied with atom probe tomography. *Angew. Chem. Int. Ed.* **55**, 11173–11177 (2016).

Acknowledgements
B.M.W. acknowledges financial support from the Netherlands Organization for Scientific Research (NWO) in the frame of a Gravitation programme (the Netherlands Center for Multiscale Catalytic Energy Conversion (MCEC), www.mcec-researchcenter.nl), as well as from the Advanced Research Center (ARC) Chemical Buildings Blocks Consortium (CBBC), a public–private research consortium in the Netherlands (www.arc-cbbc.nl). C.V. acknowledges support from a Niels Stensen Fellowship and a VATAT fellowship.

Author contributions
The authors contributed equally to all aspects of the article.

Competing interests
The authors declare no competing interests.

Peer review information
Nature Reviews Chemistry thanks D. Ma and the other, anonymous, reviewer(s) for their contribution to the peer review of this work.

Supplementary information
The online version contains supplementary material available at https://doi.org/10.1038/s41570-021-00340-y.